4. DISCUSSION OF RESULTS

The Texaco hot gas filter test program has provided baseline operating and performance data for both a cross flow and candle filter unit when integrated with an entrained gasifier. The test program has been summarized in Section 3. This section provides an evaluation of the test program findings. Filter performance, filter operating characteristics and materials durability issues are discussed.

4.1 FILTER PERFORMANCE

For oxygen blown IGCC systems the hot gas filter performance requirement is set by environmental emissions and the need to protect downstream equipment such as sorbent beds and gas turbine components. Stack emission limits and gas turbine tolerance to particle erosion may require an outlet dust loading at the filter of about 150 ppm of less than 10 μm particles (including the dilution effect of the combustion air). In the test program, the filter inlet and outlet dust loadings were measured periodically using isokinetic, total mass sampling. These results are given in Table 4.1. Cascade impactor sampling of both the inlet and outlet was also conducted by Southern Research Institute in two test runs, Tests 6 and 7. These results have been reported elsewhere.[1]

As shown by the results reported in Table 4.1, the inlet dust loadings to the filter varied over a wide range. In one test, (Test 2) an inlet loading of over 22,500 ppm is reported. This condition may have corresponded to soot blowing operations occurring in the radiant cooler upstream of the filter. The otherwise wide variation in inlet dust loading is attributed to relatively small variations in gasifier operating conditions.

Table 4.1 - Summary of Filter Performance in Entrained Gasifier Tests

Test	Filter Type/ No. Used	Hours Operation	Inlet Loading ppm	Outlet Loading ppm	Remarks
1	Cross Flow/4	58	2490 to 9109	2.2 to 6.2	- Borescope inspection showed no filter issues.
2	Cross Flow/4	35	250 to 1220 up to 22525	23 to 33 80 to 114	- Gasket seal leaks experienced on 3 filters - one filter had a delamination crack.
3	Cross Flow/4	29	270 to 2900	5 to 65	- Borescope inspection showed no filter issues.
4	Cross Flow/4	103	280 to 2866	59 to 115	- Gasket leaks on all four filters, one filter had a sheared flange.
5	Cross Flow/4	65	650 to 12,350	19 to 176	- Sheared filter flange and delamination.
6	Cross Flow/8	42	1170 to 1934	183 to 788	- Bottom filters were water soaked and damaged.
7	Cross Flow/8	60	1640	No Data	- Plugged inlet sample line. Outlet sample line was inoperable.
8	Candle/19	62	1076 to 1873	160 to 600	- Borescope inspection showed no filter issues.
9	Candle/19	34	768 to 2525	116 to 617	- Inspection showed no filter issues or dust leak path.
10	Candle/19	89	NA	NA	- Borescope inspection showed no filter issues.
11	Candle/19	101	NA	NA	- 3 Filters broken during operation.

The outlet dust loadings also varied over a relatively wide range. Test results from the initial filter operation (using cross flow filter elements) show outlet dust loadings as low as 2 to 6 ppm. These results demonstrate the performance potential of a ceramic barrier filter device to meet particulate cleanup requirements in entrained gasification applications.

In some tests, physical damage to the filter and/or dust seals were evident that would cause a breach between the dirty to clean gas side of the filter and cause increased outlet dust loading. In the later test runs it became apparent that significant contamination to the outlet gas piping had occurred that adversely influenced sampling results. Outlet loadings of several hundred parts per million were being measured (Tests 8 and 9, for example) however, inspection of the filter unit showed no evidence of any dirty to clean side breach after testing.

In addition to achieving acceptable outlet loadings, the hot gas filter must maintain a stable operating pressure drop. High system pressure drop at a nominally low face velocity and short cleaning cycles were experienced in the entrained gasification filter testing. These results suggest difficult filtration conditions indicative of high ash flow resistance, low filter permeability, and dust reentrainment.

Equation 4.1 relates the gas pressure drop through the filter media and ash cake to the filter and cake physical properties and process parameters of the operating system.

$$\Delta p = \frac{\mu V}{K_f} + \frac{\mu C V^2 \theta}{\rho_c K_c} \qquad (4\text{-}1)$$

where

μ = gas viscosity
V = filter face velocity (actual gas volumetric flow/filter area)
C = dust concentration
θ = time
ρ_c = bulk density of the dust cake
K_f = filter permeance
K_c = cake permeance

Baseline pressure drop is defined as the gas pressure drop through the filter, immediately following the cleaning event, and is represented by the first term of Equation 4.1, i.e.,

$$\Delta p_{bl} = \frac{\mu V}{K_f} \qquad (4\text{-}2)$$

The filter permeance, K_f, establishes the baseline pressure drop and may be considered a property of the conditioned filter media. It is generally accepted that in barrier filter devices, that some quantity of ash will become trapped in the surface pore structure of the filter media and become a permanent layer that contributes significantly to filter permeance. Low filter permeance leads to high baseline pressure drop with corresponding parasitic loss in cycle energy efficiency. Also, high baseline pressure drop can adversely impact the design and integrity of the dust seals and metal structures used to support the filter system. Increasing filter surface area to reduce face velocity, and therefore, pressure drop can adversely impact system economics.

The baseline filter pressure drops in the Texaco test program were directly measured by differential pressure measurements made across the filter unit. This data was summarized in Section 3 for the different filter tests. Figure 4.1 compares the filter permeance trend from the Texaco entrained gasifier filter testing with similar data from other test programs. The data is normalized by plotting the "Relative Permeance" (i.e, K_f/K_{f_o}) as a function of filter cleaning cycle. Plant

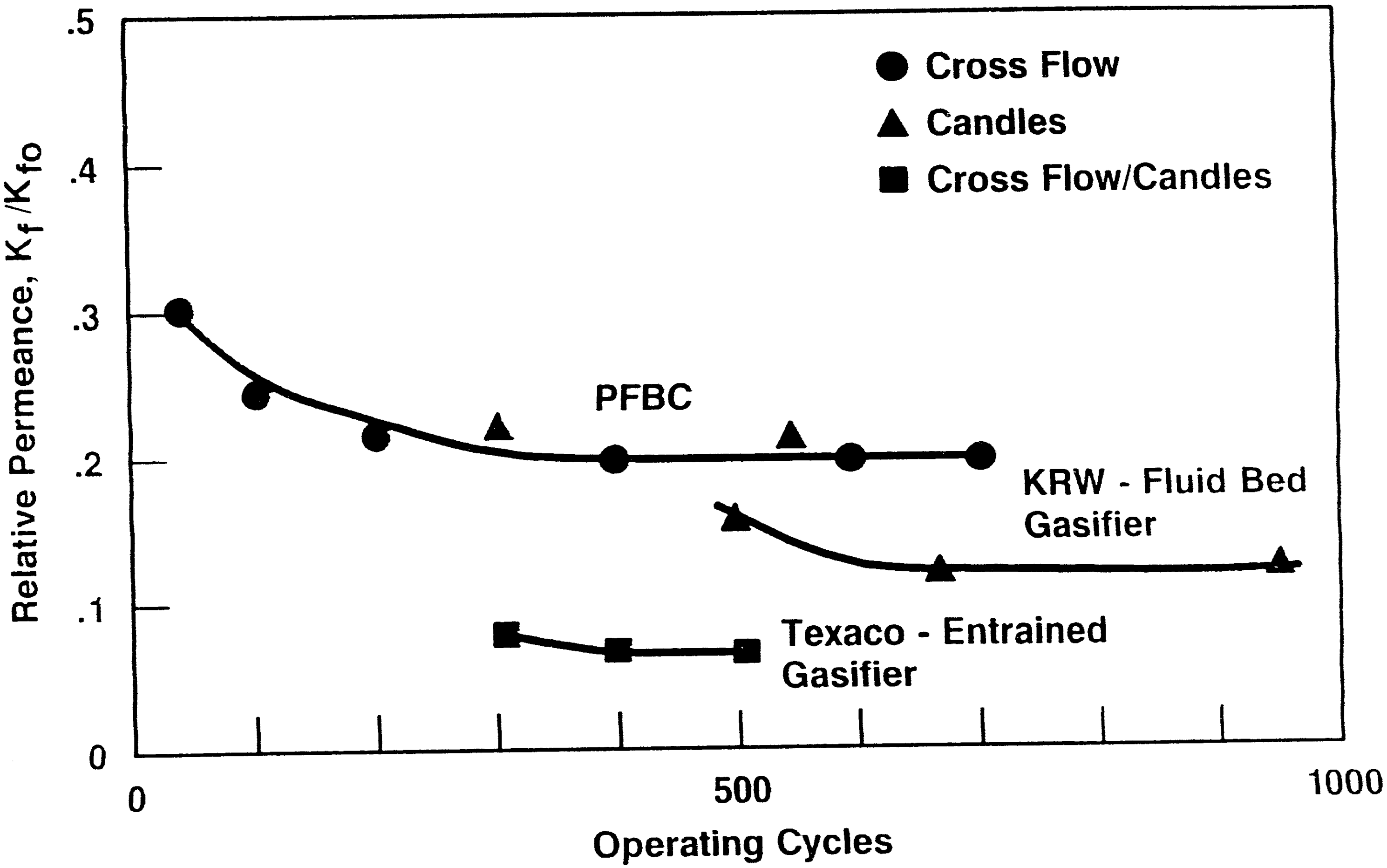

Figure 4.1 - Comparison of Filter Permeance Trends in Different Plant Applications

data is shown for typical pressurized fluidized bed combustor (PFBC) application as well as the KRW fluid bed gasification PDU. Test data include operation with cross flow and candle filters. The entrained gasifier test experience that utilized both cross flow and candle filter test units show significantly lower permeance than either the PFBC or fluid bed gasifier experiences. Low filter permeance can be the result of several factors, i.e., poor cleaning, reentrainment of fines and/or high ash flow resistance.

Both the PFBC and KRW ashes were generated in a sulfur sorbent containing fluid bed that operates at relatively low temperatures (1600°F, 870°C). Thus, the combustion and fuel gas contain both char, ash and attrited sorbent particles. The entrained gasification process occurs at over 2500°F (1370°C), generally above the ash softening point. Sulfur sorbents were not utilized upstream of the filter. Thus, in this case, the fuel gas contains primarily char and ash particles. The characterization of the entrained gasifier ash and its comparison with both the PFBC and KRW ashes are discussed in Section 4.2

Visual inspection of the test unit following some of the test runs suggest effective cleaning was occurring with the candle filters. A thin and uniform crusty layer was apparent over the candle with small, random patches of filter cake, Figure 4.2. The inspection of the cross flow filters showed mixed results. Clogging of nearly all dirty side channels was clearly evident on those filter elements that had experienced gasket or flange failures. The undamaged filters appeared cleaner with generally opened but constricted channels. The bulk of the residual ash could be easily brushed except for a thinner crusty layer that appeared to cover the filter dirty side surface.

The cross flow filter assembly used in Tests 1 through 5 contained 4-filter elements (approximately 28 ft^2 of filter surface). In Tests 6 and 7 the unit was modified to hold 8-cross flow elements (56 ft^2 of filter surface). Assuming completely "clogged" channels, the

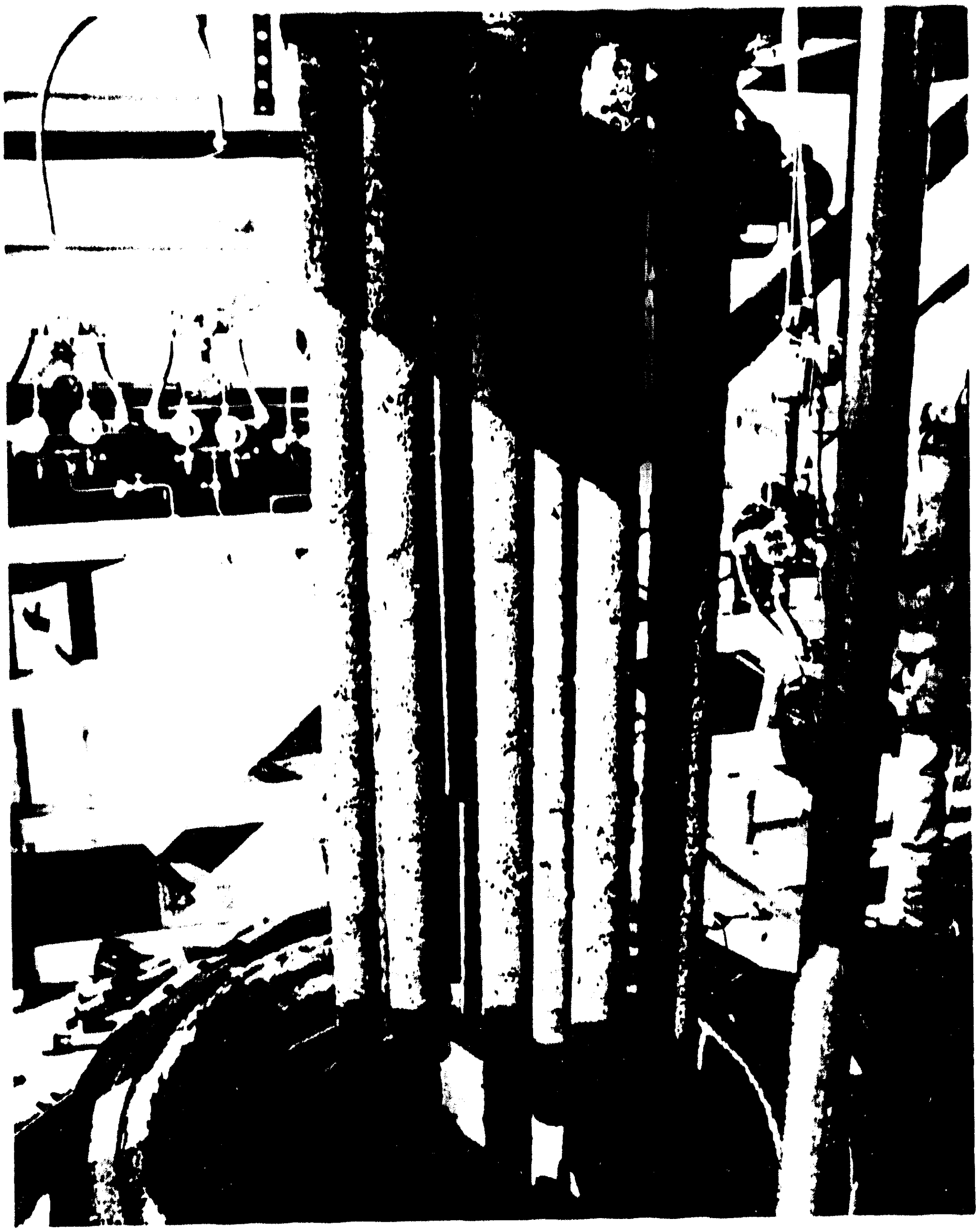

Figure 4.2 - Photograph Showing Nature of Residual Dust Observed on the Candle Filters After Test No. 9

cross flow filter surface area is probably reduced to less than 8 and 16 ft^2 for the 4 and 8 element assemblies, respectively. The candle unit contained 19 elements representing approximately 51 ft^2 of filter surface area. In view of the post test visual inspection, it could be expected that significantly higher pressure drops would have occurred during the operation of the cross flow unit. Comparison of the operating characteristics given in Section 3 shows that the cross flow exhibited similar or lower pressure drops. This suggests that the cross flow had at least equivalent active surface area as the candle unit. Therefore, it is unlikely that the clogged cross flow channels represent the condition during normal operations.

The filter permeance discussed above and shown in Figure 4.1 were based on the baseline pressure drop trend measured during test operations. Selected filter elements (both cross flow and candle) were recovered and tested in a laboratory apparatus to measure their flow permeability. The test consists of flowing a known quantity of air through the filter (with any residual dust layer) and measuring the resulting pressure drop. These results are then compared with the as fabricated filter permeability, Figure 4.3. These results show, as expected, a decrease in flow permeability (increase in flow resistance) of the used cross flow and candle filter elements. The decrease measured, however, does not account for the low filter permeance determined from the operating data. These results suggest:

1. The flow resistance of the entrained gasifier ash under ambient conditions is significantly lower than under process gas environment and temperature,

2. Significant reentrainment or poor cleaning are occurring under process conditions that effectively mask the actual baseline pressure drop.

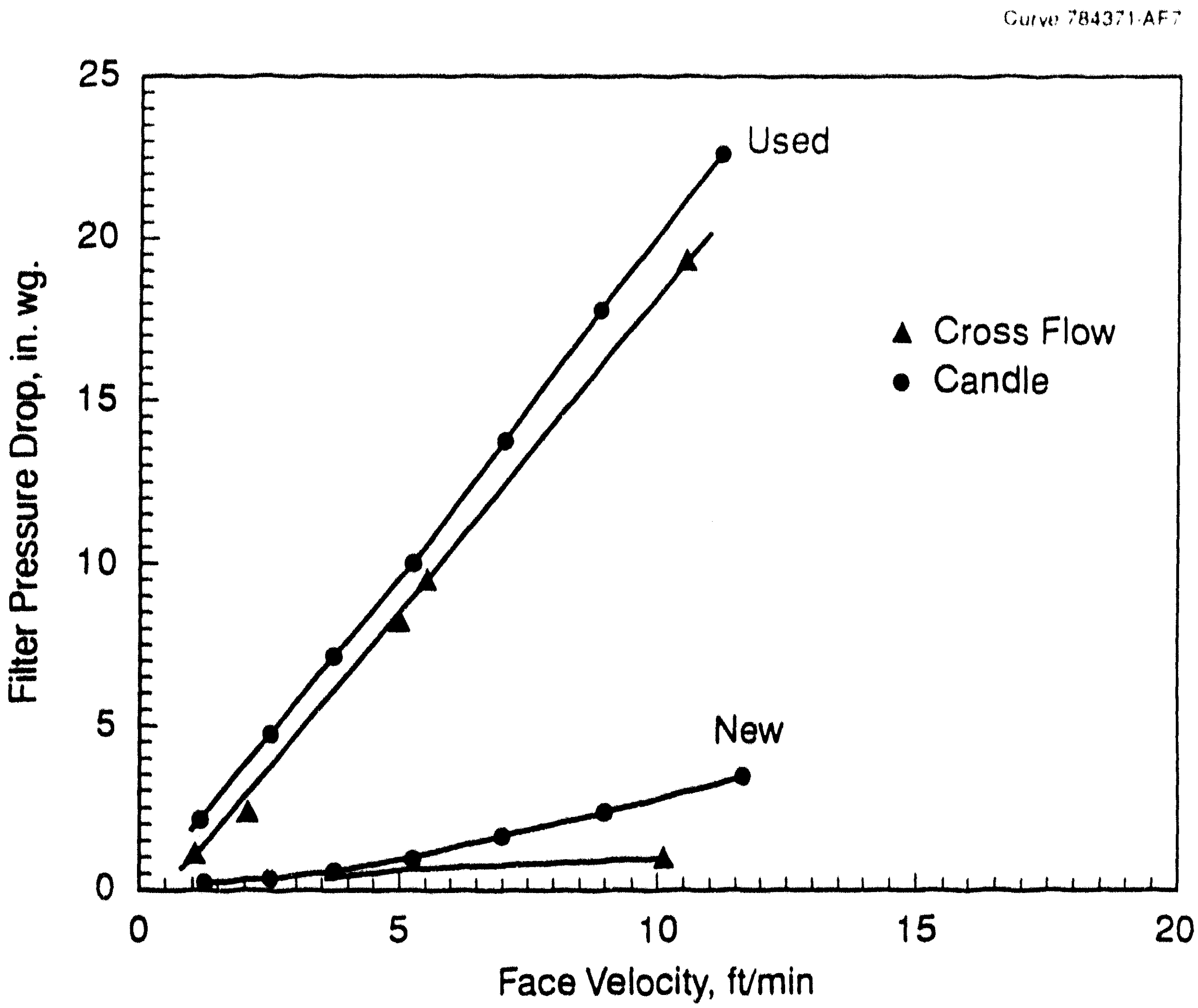

Figure 4.3 - Comparison of Flow Permeability of Used (Texaco) and Unused Filter Elements

The poor cleaning scenario is not, however, consistent with the candle filter inspection observations. Low ash flow permeability and its potential for reentrainment would appear to be the primary factors in establishing filter operating pressure drop characteristics in this test program.

4.2 CHARACTERIZATION OF ENTRAINED GASIFIER ASH

A range of test and measurement methods were used to characterize samples of the collected filter ash catch from the entrained gasifier testing. The testing has included cascade impactor sampling[1] and laboratory ash analysis (Appendix B) conducted by Southern Research Institute (SRI) and off-line filter testing conducted by Westinghouse. A brief summary of the ash characterization studies is presented.

Sedigraphic analysis, Figure 4.4, based on samples from Test Run 1, show a substantial weight fraction (about 8%) of particles in the particle size range of less than 1.5 μm. Over 14% of the mass in this sample is below 2.3 μm. The large fraction of particles in the 10 to 30 μm range that is also present is not surprising in this sample since in Test No. 1 there was no precleaning cyclone ahead of the filter unit. The high entrainable fines fraction may be an important factor in the high baseline pressure drop observed. With repeated cleaning cycles, the very small fines reentrain and deposit back on the filter. These fines form a thin, highly resistive and adhesive layer of concentrated fines that is not easily dislodged during subsequent pulse cleaning.

Other laboratory data were developed that generally reflect on the pressure drop characteristics of the filter cake. Two of these parameters are the Drag-Equivalent Diameter and Cake Resistance. The Drag Equivalent Diameter is not a measurement of physical size, but rather a fitted parameter ranking the characteristic gas flow resistance

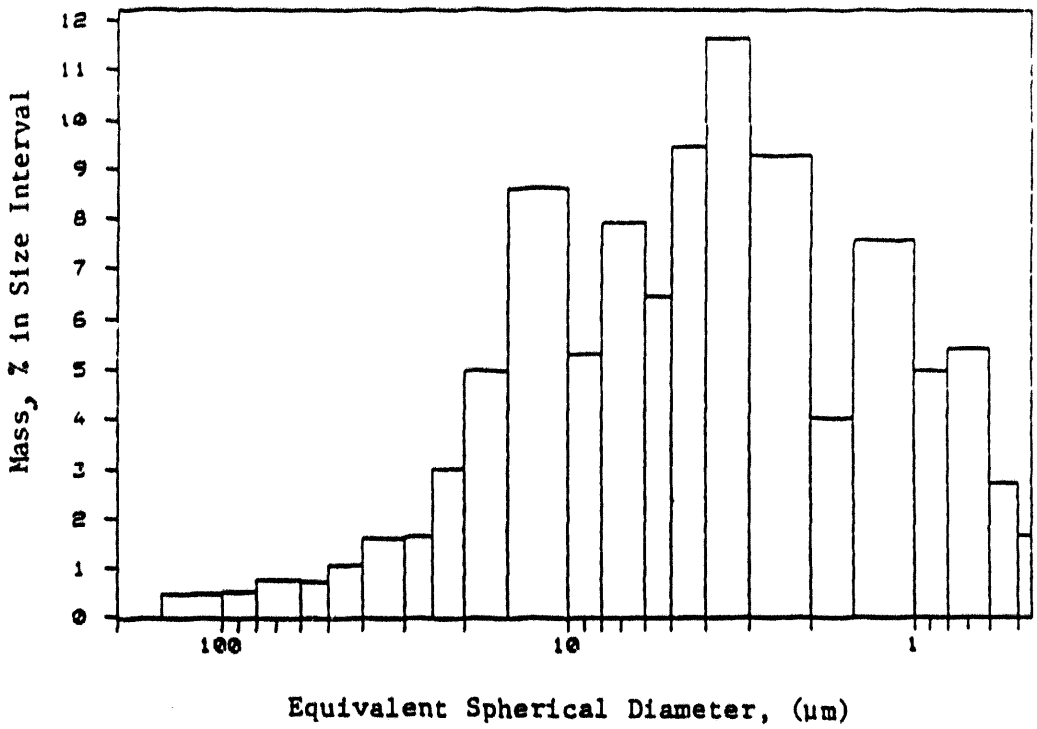

Figure 4.4 - Mass Population for Texaco Ash Sample (Test No. 1)

of ashes at equal porosities. Increasing values indicate a lower cake resistance. The drag equivalent diameter for the Texaco ash sample was 0.621 μm. SRI reports that this value is quite low (high cake resistance) when compared to PFBC or conventional pulverized coal boiler (PC) ashes. SRI provides a more general comparison of gasifier, PFB and PC ash characteristics.[2] These results in general support the high pressure drop characteristics observed in the entrained gasifier filter testing.

A direct measurement of cake resistance was also developed by feeding reentrained ash material at process conditions (T, P) and collecting the ash on the actual filter media. This approach reproduces flow conditions, but does not reproduce gas-phase compositions. Table 4.2 provides a summary of the Texaco ash characterization and compares this with similar data for fluid bed gasification and PFBC ashes. These results show that filter cake flow resistance increases with decreased particle size and is significantly higher for the tested gasification ashes, consistent with the SRI laboratory analysis.

The possibility of pore pluggage by the gasifier fines through the wall of the filter causing high pressure drop was also investigated. SEM and microprobe analysis of used filters were conducted. These results showed an accumulation of the gasifier ash fines along the dirty gas channels but typically limited to within only the first 100-200 μm (2 or 3 pore layers) of the filter matrix. A much smaller quantity of ash was also found deeper into the filter wall. These fines appeared attached to the amorphous (glass) phase of the cross flow mullite structure, but did not appear to cause any significant pore blockage. Based on these results, it is concluded that in-depth filter wall pluggage by fines was not a contributing factor in the high pressure drops encountered in the filter tests on the Texaco entrained gasifier. In general however, this test program was too short in duration to establish any long term effects of fines accumulating in the filter pores.

Table 4.2 - Comparison of Ash Characteristics for Gasification and PFBC

Parameter	Texaco Ash Sample	KRW Ash Sample	PFBC Ash Samples		
			Course	Nominal	Fine
Mean Dia., μm	4.5[1]	3.5	9.7[1]	3.6[1]	2.4[1]
Bulk Density (lb/ft^3)	8 - 15				
Drag-Equivalent[1] Diameter, μm	0.62	0.46	1.25	.87	0.35
Flow Resistance ($1/ft^{-2}$)$\times 10^{10}$	110	130	7	18	26

(1) From SRI Sample Analysis

The issue of dust cake reentrainment has been extensively investigated for conventional pulse jet baghouses.[3] The potential for reentrainment in the filter in gasifier application is seen by comparing the relevant process and cake properties as shown in Table 4.3. The low bulk density and large fraction of fines present appear to provide favorable conditions for reentrainment. Test experience suggests that PFBC ashes are cohesive and when pulse-cleaned from the filter maintain relatively large agglomerates with low entrainment potential. Under ambient conditions, the entrained gasifier ashes visually appear noncohesive although some property parameters (uncompacted bulk porosity) suggest otherwise (see Reference 2). If the entrained gasifier ash is truly noncohesive, the large agglomerates when pulse cleaned from the filter may be redispersed to form reentrainable fines.

The possibility of reentrainment with high ash resistance in the entrained gasifier application was recognized early in the Texaco test program, and design modifications were implemented in an effort to circumvent these potential issues. Two basic changes were made to the filter unit following Test No. 5. The first modification was to reduce filter face velocity by doubling filter surface area. The number of cross flow filter elements were increased from 4 to 8. This was equivalent to a four-fold increase in the time between cleaning cycles, which was ranging from 0.5 to 2 minutes. The second modification involved the implementation of a cylindrical coaxial shroud. The purpose of the shroud was three-fold; to distribute the incoming solids and gas stream in an axisymmetric manner; to decelerate the gas in the annulus region between the shroud and liner; and to allow the gas to enter the filtration zone in a top-down flow orientation. The predominantly downward flowing gas would promote the settling of the dislodged dust cake fragments thus reducing the extent of redeposition. The above described modifications were utilized in the cross flow Tests No. 6 and 7. Unfortunately, both test runs experienced other operating

Table 4.3 - Comparison of Filter Duties

	Cold End Baghouse	PFBC	IGCC
Pressure, psia	15	215	365
Temp, °F	300	1600	1200
ρ_{gas}, lbs/ft^3	0.05	0.2	0.4
ρ_{solids}, lbs/ft^3	60	60	10
ρ_{solids}/ρ_{gas}	1200	300	25
Reentrainment Potential	Low	Moderate	High

problems that prevented quantitatively evaluating the modifications. It did appear in Test No. 6 that somewhat longer filtration cycles were achievable. In this test, pulse cleaning frequencies ranged between 4 to 6 minutes compared to the sometimes less than 2 minutes experienced in the earlier test runs.

Although the actual entrained gasifier test runs could not conclusively confirm the expected advantages of the coaxial shroud, the rationale for its implementation was evaluated in a full scale, Plexiglas model. The model contained two plenum sections each with five cross flow elements, very similar to the actual Texaco filter installation. A summary of this work is given in Section 4.3 below.

4.3 COLD FLOW MODELING OF CROSS FLOW FILTER

In support of the filter design modification implemented in the Texaco cross flow filter unit, cold flow testing was conducted to simulate the modified configuration at full scale. The cold flow model, shown in Figure 4.5, consists of an air blower, two cross flow filter plenum modules, a transparent Plexiglas vessel that houses the filter assembly, a dust injection system, a filter pulse-back system, and instrumentation and data acquisition. The cold model facility was built and operated in support of another DOE contract. A complete description of its design and operational capabilities is provided in Table 3.2.[4] The cold model is used for:

- System flow and pressure drop measurements
- Flow visualization using smoke and/or dust
- Flow field velocity profile and pattern using anemometers
- Comparison of alternative gas shrouding and/or inlet configuration
- Distribution of the pressure pulse during cleaning
- Visualization of the filter pulse cleaning event showing cake removal
- Measurement of flow and pulse cleaning induced vibration using accelerometers.

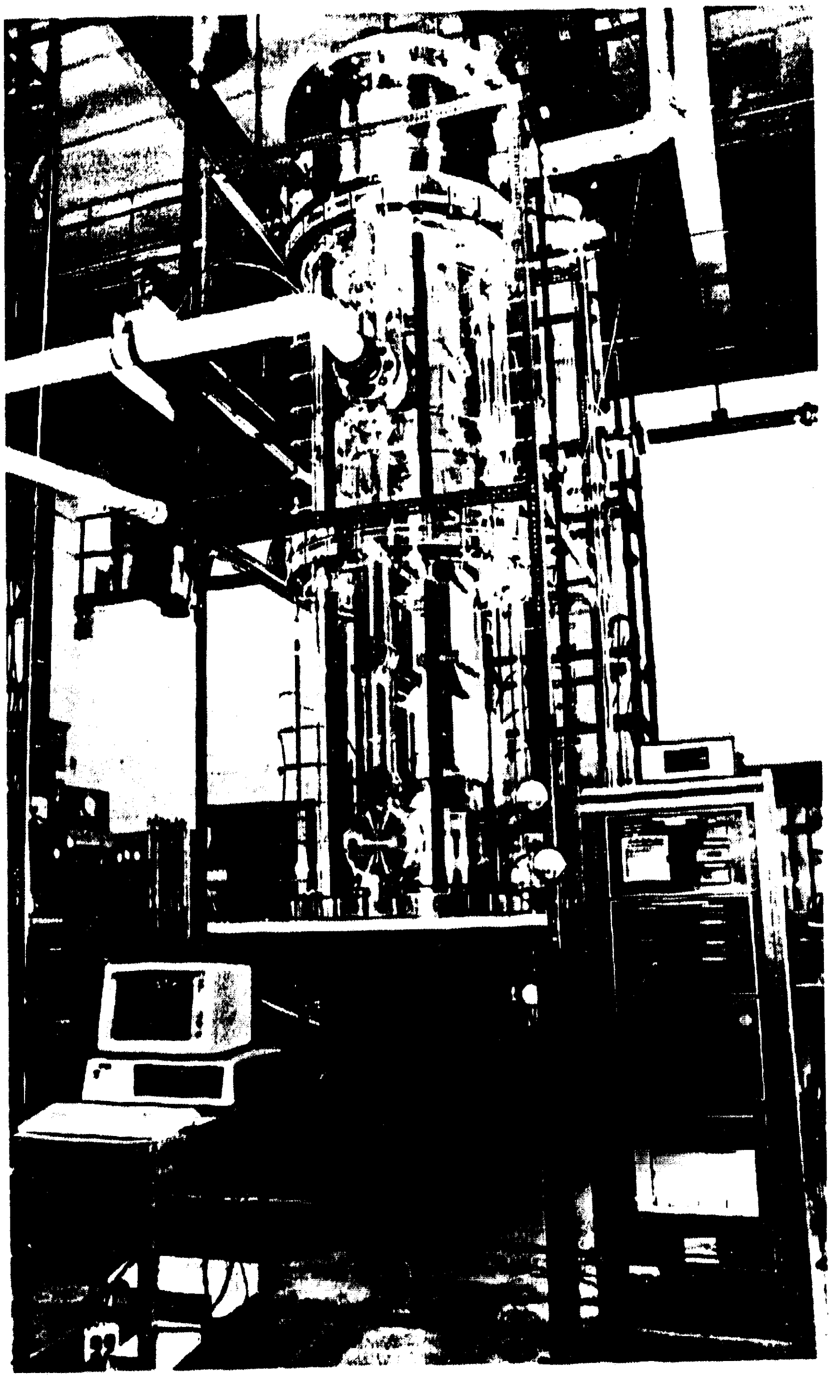

Figure 4.5 - Photograph Showing Full Scale Cross Flow Filter Cold Flow Model with Coaxial Shroud

The mathematical basis for the valid simulation of the flow and vibration characteristics under cold flow conditions is provided in Reference 4.

Utilizing the radial gas inlet port with a coaxial shroud simulating the modified Texaco filter configuration, flow visualization studies using smoke injection and the measurement of the flow velocities were conducted. Figure 4.6 shows a schematic representation of the observed flow field pattern. In general, the gas was observed to distribute uniformly across the top of the shroud and maintain a downward orientation over the length of the shroud. Below the shroud, a gentle downward flow was observed at near the vessel wall with a clockwise swirl that had a velocity component that ranged from 0.5 to 4 ft/s depending on the inlet gas flow rate (100 to 400 acfm). The downward component of the flow formed an annular region that was approximately 10 inches wide extending inward from the vessel wall. The annular region represented about 75 percent of the superficial area of the vessel internals. Starting beneath the shroud region, there also was a gas upflow between the two filter plenums that had a velocity component that ranged below 1 ft/sec. Below the filter plenums and in the ash hopper the gas appeared to be stagnant.

Flow vibrational measurements were also conducted using the cold flow test facility. Vibrational measurements were conducted by attaching two accelerometers to the outside surface at the bottom (lowest) of one plenum. This arrangement allowed measurement of vibration in two horizontal directions, one perpendicular and one parallel to the surface of the filter flow channels. Three different vibrational tests were performed:

- Normal gas flow alone
- During pulse cleaning - no flow
- Gas flow with pulse cleaning.

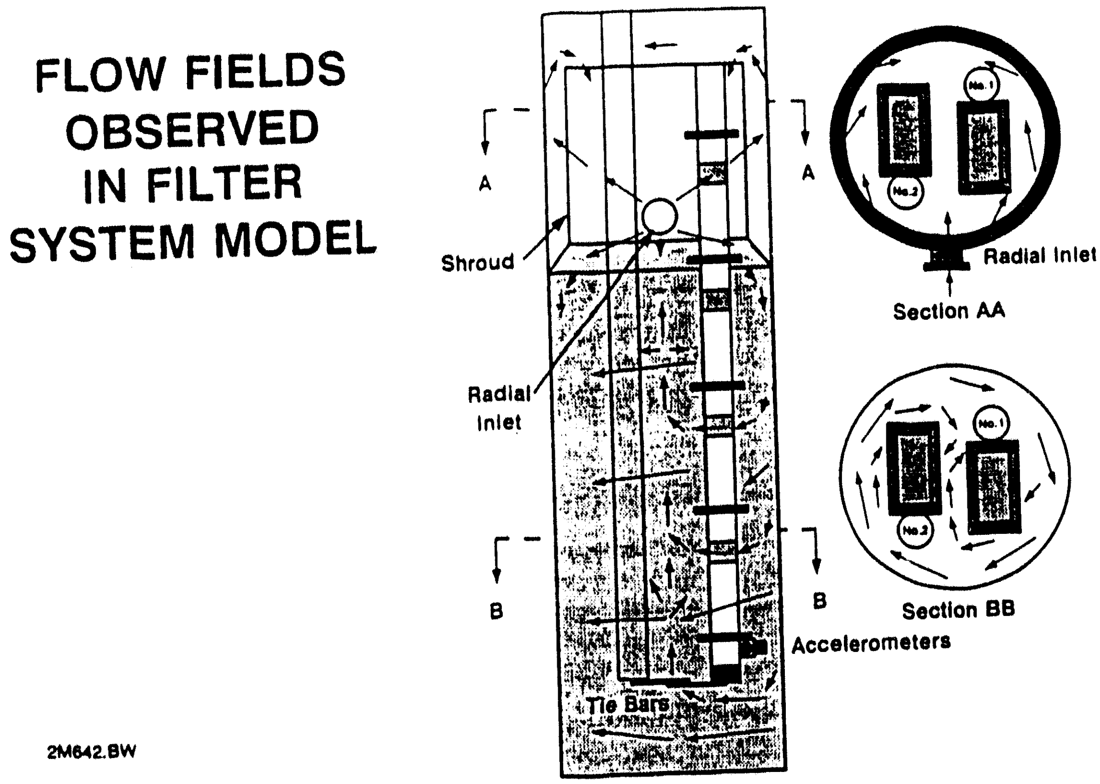

Figure 4.6 - Flow Fields Observed in Filter System Model

During the normal gas flow period, the accelerometer data showed little or no low frequency pendulum-type vibration. An acceleration peak of only 0.04 g's was measured.

For the pulse cleaning vibrational test, pulse tank pressures were varied from 40 to 200 psi with the pulse duration varying from 0.1 to 0.2 seconds. Vibrational inner action effects between the two plenums was also investigated including the case of coupled and uncoupled plenums (bottom braced). Plenum accelerations induced by the back-pulse event ranged in the order of 10 to 20 g's in the direction perpendicular to the filter surface and varied with pulse tank pressure. No appreciable difference in vibration intensity was observed when the two plenum modules were coupled. Stresses imposed on the filter due to the observed accelerations and frequencies were estimated to be no more than about 50 psi if uniformly distributed over the filter flange surface. Vibration induced by pulse cleaning is therefore not expected to cause filter element failure unless coupled with other stresses. Vibration could however promote the rapid transmission of a small crack once formed by other mechanisms.

4.4 FILTER UNIT DURABILITY

Testing on the Texaco entrained pilot plant gasifier facility exposed the hot gas filter to a wide range of operating and upset conditions. Both cross flow and candle filter elements were damaged in one or more of the tests. In the early cross flow testing, the dust seals (gaskets) used in the filter mounting to the plenums failed resulting in dust leaks and perhaps contributing to filter failures.

Table 4.4 provides a listing of the cross flow filters used, exposure hours and failure mechanism observed (if any). The filters lost in Tests 6 and 7 are shown but should be discounted because of the facility upsets that occurred (see Section 3) that likely caused (or significantly contributed to) the failures. In Tests 1 through 5, a total of 9 cross flow filters were utilized.

Table 4.4 - Summary of Cross Flow Filter Usage

Filter Identification	Test	Type Failure	Operating Hours
2	1,2,3,4	None	215
WRTX 12	1,2,3,4	None	215
13	1,2,3,4	None	215
14	1,2	Delaminated	83
4	3,4	Failed Flange	132
15	5	None	65
16	15	Delaminated	65
17	5	Failed Flange	65
18	5	None	65
44	6	None	42
46	6	Delaminated	42
47	6,7	See Note 1	102
49	6,7	See Note 1	102
51	6	Delaminated	42
54	6,7	See Note 1	102
55	6,7	See Note 1	102
50	7	See Note 1	60
52	7	See Note 1	60
83	7	See Note 1	60
86	7	See Note 1	60

Note 1 - Operational Events

Test 6 - Water found in lower filter plenum
- 100 gal water recovered from ash hopper.

Test 7 - Significant thermal transient on startup
- Temperature and flow fluctuations experienced
- Rapid depressurization
- Broken tubesheet

Five of these filters were not physically damaged. Two of the four damaged filters suffered cracked flanges. The other two filters experienced delamination only. Inspection of the delaminated only filters showed evidence of only very little ash breaching through the delamination crack. Delaminations are believed to be the product of weak bonding of the filter plates during manufacturing and could be eliminated if a monolithic cross flow structure is developed.

Coincidentally with the occurrence of the cracked flange in the Texaco filter unit, two similar failures had also occurred in the Westinghouse test facilities after over 1300 hours of operation at 1550°F under simulated PFBC conditions. As part of this in-house program, Westinghouse undertook a redesign of the filter mount. The modified mount design was backfitted into the simulator testing at Westinghouse and the filter unit at Texaco. Analysis showed the original mount suffered from three principal deficiencies:

1. Nonuniform loading of the ceramic flanges imparting point or line stresses and large bending moments,

2. Relaxation of the filter clamping bolts causing excessive loosening of the mount, and possible levitation of the ceramic element during reverse pulse cleaning, and

3. Wedging of dust in the cavities outside the filter element seating area that caused high stresses due to differential contractions during shutdown periods.

A modified and improved clamping design was developed that corrected these identified deficiencies. The design is described in the Long Term Durability Final Report.[5]

In addition to the mount redesign, a redesign of the gasket used for the dust seal was also made. The original dust seal used in the Texaco filter unit utilized an 0.15 inch thick Interam® Brand Mat made by the 3M Company. This material is made of alumina silicate fibers interspersed with an intumescent or heat expandable layer of vermiculite. This material shows low mechanical strength and has limited temperature capability before losing its intumescent property. In the Texaco entrained gasifier application, high pulse gas intensity (10 to 20 psi) is required because of the high resistance of the ash cake. With these high back pressures, these seals are prone to erode if the reverse pulse gas flows through the seal joint. To circumvent the use of this relatively weak and temperature limited seal, Westinghouse developed a Nextel-reinforced Interam MM Fiber Blanket seal that was also backfitted into the Texaco filter unit subsequent to Test 5. This seal design is significantly resistant to erosion or blowout.

In Tests No. 6 and 7 the retrofit mount and dust seal were implemented. As described earlier, severe plant upsets occurred and several filters were broken in Test 6 and all filters broken in Test 7. Of the eight filters in Test 6, three failed. None of the filters failure, however, involved either a flange crack of the earlier type or eroded dust seal. In Test 7, damage to the filter bodies was extensive including some flange breakage. However, no dust seals were lost.

One cross flow filter which had operated during Tests 1 and 2 has been subsequently characterized for material strength. Bend bar samples were cut from the thin wall gas channels. These results showed a slightly lower strength (<5%) over similar samples taken from a filter of the same fabrication lot. This difference may not be statistically significant. Comparison of bend bar samples taken from the flange region of the as fabricated and used filters showed no strength difference. Thus, short term exposure of the alumina/mullite cross flow filters to the entrained Texaco gasifier fuel gas did not result in any significant material strength degradation.

In Tests 8, 9, 10 and 11, a nineteen (19) element candle array was utilized. Seventeen (17) of the candles were the silicon carbide F40 Dia Schumalith, (1.5 meter long) and two candles were a first generation Coors alumina/mullite, (1 meter long). A borescope inspection after Test 8, a visual inspection (unit disassembly) following Test 9, and a borescope inspection after Test 10 revealed no failed filters. After Test 9, one candle was removed and the seal inspected. No dust leak was evident. Following Test 11, the filter unit was disassembled and then inspected. Three candles were broken (one of the SiC's and both of the developmental alumina/mullite elements). A second SiC candle broke when attempting to remove it from its mount. It was evident from the increased pressure drop through the Texaco sorbent beds that at least one candle had failed about midway through the test period.

4.5 CHARACTERIZATION OF FILTER MATERIALS

4.5.1 Cross Flow Filters

The alumina/mullite matrix used in the manufacture of cross flow (and candle) filters consists of 60 to 70% mullite ($3Al_2O_3 \cdot SiO_2$) and 3-5% alumina (Al_2O_3) with varying concentrations of the amorphous and anorthite ($CaAl_2Si_2O_8$) phases. In general, when exposed to the entrained gasifier reducing gas process conditions, a crystallization of the amorphous phase will occur forming additional anorthite. Mullitization and/or recession of the amorphous phase of the alumina/mullite matrix also occurs that can alter the general appearance of the pore structure. The long term effects of these phase changes are yet unknown.

The characterization of the physical, mechanical and microstructural properties of one cross flow filter that had been exposed in the Texaco gasifier testing has been reported.[6] Results of this work show that the room temperature flexural strength of the filtering surface of the cross flow element decreased only very slightly (~5%) after 77 hours exposure to the entrained gasifier environment. However, a moderate decrease in the Weibull modulus (14 to 9) was measured for the exposed filter suggesting a possible change (increase) in its flaw population. Microstructural investigations, which included SEM and EDAX analysis, revealed no substantial physical changes to the filter as a result of the testing nor the presence of any chemical or phase changes not anticipated based on the process gas conditions.

4.5.2 Candle Filters

In the Westinghouse high temperature, high pressure (HTHP) particulate removal system which operated at the Texaco gasification facility in Montebello, California, two 1 m P-100A alumina/mullite and seventeen 1.5 m clay bonded silicon carbide F40 candles were subjected to ~400 hours of operation in the 700°C reducing gas environment. After testing was completed, both P-100A alumina/mullite filters had fractured near or within the flange holder, while only one clay bonded silicon carbide F40 candle failed also near the flange. During shipment to Westinghouse, the clay bonded silicon carbide F40 candles fractured into numerous segments. A reduction in material strength of the clay bonded silicon carbide matrix was evident not only in the fragility of the exposed candles during transport, but also in the retention of only ~65% of the full candle 4-point flexure strength after operation in the Texaco gasification environment.

Sections of the P-100A alumina/mullite and clay bonded silicon carbide F40 candles that were retrieved from the ash hopper were subjected to room temperature and process temperature strength characterization (i.e., C-ring compression and tension testing). As shown in Table 4.5, the as-fabricated room temperature strengths of the P-100A alumina/mullite and clay bonded silicon carbide F40 candles were nearly comparable. The initial hot strength of the P-100A alumina/mullite matrix appears to be marginally stronger in comparison to the clay bonded silicon carbide F40 matrix.

Table 4.5 - Bulk Material Strength

			Room Temperature C-Ring		Hot Strength C-Ring	
Candle ID	Temp., °C	Time, Hrs	Compression, psi	Tension, psi	Compression, psi	Tension, psi
Alumina/Mullite (P-100A)						
C-9	---	---	1938±179	1855±201	2203±215 (1)	2815±416 (1)
C-19	700	400	703±377	558±303	676±352 (2)	839±454 (2)
Clay Bonded Silicon Carbide (F40)						
S/APF-153	---	---	1300±213	1907±111	1416±127 (3)	2328±228 (3)
S/APF-135	700	400	1103±146	1063±218	1068±121 (4)	1653±249 (2)

(1) Hot Strength Tested At 870°C.
(2) Hot Strength Tested At 700°C.
(3) Hot Strength Tested At 732°C.
(4) Hot Strength Tested At 800°C.

After exposure in the 700°C reducing gas environment, the P-100A alumina/mullite matrix experienced a relatively uniform loss of room temperature bulk material strength. Only 30-36% of the initial P-100A alumina/mullite strength (i.e., ID and OD strength, respectively) was retained in the material. The low retained strength in the P-100A (alumina/mullite) candle filters appear in sharp contrast to the high (~95%) retained strength of the cross flow reported in Reference 7 (summarized above). A direct comparison, however, is cautioned due to difference in conditions of the actual test runs, filter configuration, and processing and material test methods (bend bar vs C-ring).

In contrast, the clay bonded silicon carbide F40 matrix retained ~85% of its as-manufactured bulk strength along the candle OD surface, while ~56% along the candle ID surface. The influence of pulse cleaning appears to have induced moderate thermal fatigue as evidenced by the lower ID strength in the clay bonded silicon carbide F40 matrix in the gasification environment. Note that since both of these materials were sections that had failed and fallen into the ash hopper, we suspect that the bulk material strengths shown in Table 4.5 reflect the catastrophic failure events that the candle matrix experienced.

As shown in Table 4.5, the hot strength at 700°C is comparable to the reported room temperature strengths for both the P-100A alumina/mullite and clay bonded silicon carbide F40 filters that were exposed to the reducing gas environment. As with room temperature strength, the P-100A alumina/mullite matrix underwent a significant loss of process temperature bulk material strength, in comparison to a somewhat greater retention of the initial bulk material strength in the clay bonded silicon carbide F40 matrix at comparable test conditions.

Note that with the exception of the Texaco-exposed P-100A alumina/mullite matrix, all tested samples have a 10-20% 1σ variation in bulk material strength. The significant variation (i.e., 50%) indicated for the P-100A alumina/mullite material implies a lack of homogeneity within the candle body after exposure to the Texaco gasification conditions.

In an attempt to identify changes that occurred within the microstructure of each material, sections of both the Texaco exposed P-100A alumina/mullite and clay bonded silicon carbide materials were subjected to scanning electron microscopy/energy dispersive x-ray analysis (SEM/EDAX). Characterization of the clay bonded silicon matrix after exposure in the Texaco gasification environment indicated that $<5-10\ \mu m$ nearly spherical droplet formations resulted along the binder coated grains that were directly beneath the fibrous candle OD membrane. The droplet formations were identified to be compositionally similar to the binder phase (i.e., silicon, aluminum, potassium, and sodium). Perhaps either carryover of liquid aerosol droplets from the gasifier or sorbent bed resulted along the surface of the clay bonded silicon carbide grains, or outgassing of the underlying substrate occurred.

Typically micron and submicron-sized ash fines were detected along the clay bonded silicon carbide surface. At these locations mullite-like rods and whiskers were evident, indicating that crystallization of the binder matrix had resulted during the high temperature exposure in the Texaco gasification environment.

Further crystallization of the binder phase was evident along the ID surface of the clay bonded silicon carbide filter matrix that was exposed to the Texaco gasification environment. The mottled surface appearance of the ID binder phase was uncharacteristic of the mullite whisker- or needle-like formations that were observed along the OD surface. Further effort is needed to identify the resulting phase and possible impact of pulse cleaning on the binder phase transitions.

Iron was frequently detected in localized areas along the binder/grain interface. Iron which is initially present in the as-manufactured clay bonded silicon carbide matrix, conceivably migrated to the grain interface during filter operation. The interaction of iron with the adjacent silicon carbide grain could potentially lead to the formation of an iron silicate complex (i.e., $FeSiO_3$ or Fe_2SiO_4). The relatively low operating temperatures of the Texaco gasification system (i.e., 1300°F) are substantially below the the melt temperatures of either iron silicate complex (i.e., ~1140°C; ~1500°C, respectively).

Characterization of the Texaco exposed alumina/mullite filter matrix was conducted along the flange areas of the candles that were initially returned to Westinghouse. In comparison to the as-manufactured matrix, mullitization and/or recession of the amorphous phase in the alumina/mullite matrix was evident.

4.6 REFERENCES

1. Nakaishi, C. V., P. C. Yue and W. E. Farthing, "Particle Characterization from a Sub-Pilot Scale Entrained-Bed Gasifier," paper presented at the Ninth Symposium on the Transfer and Utilization of Particulate Control Technology, Williamsburg, VA, October 15-18, 1991, .

2. Pontius, D. H., "Characterization of Particles Emitted in Gasification and Combustion Processes," paper presented at the Second EPRI Workshop on Filtration of Dust From Coal-Derived Reducing and Combustion Gases at High-Temperature. San Francisco, CA, March, 1992.

3. Leith, D., and M. W. First, "Filter Cake Redeposition in a Pulse-Jet Filter," EPA-600/7-77-002, 1977.

4. Robertson, A., et al., "Second Generation Pressurized Fluidized Bed Combustion Plant - Conceptual Design and Optimization of a Second Generation PFB Combustion Plant - Technical Progress for Phase 2, October 1, 1990 through September 30, 1991 - Prepared by Foster Wheeler Development Corporation under DOE Contract DE-AC21-86MC21023.

5. Lippert, T. E. and E. E. Smeltzer, "Long Term Durability Testing of Ceramic Cross Flow Filter," - Final Report DOE Contract DE-AC21-87MC24022, 1992 - Pending Publication.

6. Singh, J. P., et al., "Materials Qualification Technology of Ceramic Cross Flow Filters," ANL/FE-91/1.

5. SUMMARY AND CONCLUSIONS

The performance and durability of a hot gas, cross flow filter system was evaluated while integrated with the operation of the Texaco 15 tpd, entrained-bed gasifier pilot plant facility that is located at their Montebello Research Facilities (MRL) in California. A candle filter unit was also tested for comparative purposes. The gasifier operates at a system pressure of 350 psig under either oxygen or air blown conditions, producing a maximum fuel gas flow to the filter system of 120 acfm. Except for the initial filter commissioning test, all the hot gas filtration tests were conducted in conjunction with Texaco's prime contract with DOE/METC which focused on exploring and demonstrating advanced hot gas desulfurization technology. This work included use of external sorbent beds downstream of the hot gas filter. In the Texaco test program, the hot gas filter unit was positioned between the gasifier and the sorbent bed, and used to filter the hot (1000 to 1500°F) particle laden fuel gas carried from the gasifier through the radiant cooler section. The filter therefore, protected the sorbent beds from plugging due to excessive ash carryover. In a commercial IGCC power plant, the hot gas filter would also protect the gas turbine component from particle erosion and provide sufficient particle removal to meet environmental emission requirements.

In the MRL facility, tests were conducted in both the oxygen and air blown mode and some tests included a precleaning cyclone upstream of the filter. Test flexibility was provided by including a bypass leg around the filter unit. These process and configuration alternatives provided a relatively wide variation in the filter inlet dust loading and gas temperature conditions. Eleven separate test runs were conducted utilizing the Westinghouse hot gas filter system integrated with the Texaco gasifier operation. The test program was initiated in April 1989 and concluded in August 1992.

The first five test runs utilized a 4-element cross flow configuration accumulating approximately 280 hours of operation. This test series included operation with and without the precleaning cyclone and in two tests the sulfur sorbents were injected upstream of the filter unit. The filter operated over a range of gas flows corresponding to a filter face velocity ranging from about 2 to 4 ft/min. Nine different cross flow elements were utilized in this test series. The mounting flanges on two of the filters were damaged. Erosion of the dust seals and dust leakage through the seals was also evident.

In test runs 6 and 7, accounting for approximately 102 hours of operation, the cross flow unit was upgraded to an 8-element configuration and included a modified dust seal and flange mounting arrangement. Operating face velocities were reduced to between 1 to 2 ft/min. The precleaning cyclone was used in Test 6. In Test 7 no cyclone was utilized, but both iron oxide and calcium based sorbents were injected upstream of the filter. In both tests, upsets in the operation of the facility produced conditions in the filter unit that lead to damaged filter elements.

Tests 8 through 11 used a 19-element candle filter array that was operated for approximately 286 hours. Seventeen of the candles were the 1.5 m clay bonded Schumacher Dia Schumalith elements, two candles were 1 m long, first generation Coors alumina/mullite elements. In this test series, only the external sorbent beds were utilized and there was no precleaning cyclone directly upstream of the filter. With the 19-element candle array, the filter unit operated at a nominal face velocity ranging from 1 to 2 ft/min. Three candle elements were apparently broken during Test Run no. 11.

Based on the test program conducted, the following overall results and conclusions are made:

- The performance potential of the cross flow filter was demonstrated during the initial test runs. Outlet particle loadings ranging between 2 to 6 ppm were measured which are significantly below any environmental or gas turbine requirement.

- Visual inspection of the filter gasket seals and tubesheet, in lieu of outlet sampling, proved to be a more reliable means of evaluating filter dust collection performance. The outlet sampling was unreliable because of ash contaminating the piping system once a filter failure had occurred.

- Candle filter performance potential was demonstrated in Test Runs 8 through 10. Following Test Run 10, the candles and respective dust seals were inspected and found to be in excellent condition with no obvious breach having occurred between the dirty and clean gas sides. A failure in the candle unit occurred in Test Run 11.

- Characterization of the entrained gasifier ash shows high flow resistance, low bulk density and high fines (<2 μm) fraction. These properties provide for high reentrainment potential for noncohesive ashes. Careful characterization of gasifier ashes is required to properly design and size a barrier filter unit for IGCC power plants.

- Both candle and cross flow filter units showed pressure drop characteristics that appear significantly different than fluid bed combustion experience. Thus, the high baseline pressure drop and high cleaning frequency experienced in the initial cross flow testing are not unique to the cross flow geometry, but indicative of the entrained gasifier application (i.e., high cake resistane and significant reentrainment).

- The precleaning cyclone had little effect on the filter system operating characteristics.

- Although filter pore pluggage by gasifier fines was not a significant factor in filter degradation in this testing, longer term operation will be required to confirm this conclusion.

- Both cross flow and candle filter elements were damaged in respective testing. The damaged cross flow elements included both delamination and cracking of the mounting flange. A redesigned filter mounting system and dust seal was implemented that appeared to correct the flange and seal erosion problems. The delamination cracks experienced in some of the cross flow filters in the Texaco testing did not appear to seriously compromise performance (based on appearance of the dust tracks) but remain to be corrected through improved manufacturing and inspection procedures. Candle filter breakage did not appear to be attributable to the mounting arrangement since the breakage occurred well below the candle holder assembly.

APPENDIX A

Westinghouse Hot Gas Filter Test Unit

Mechanical Drawings
and
Process and Instrumentation Diagrams

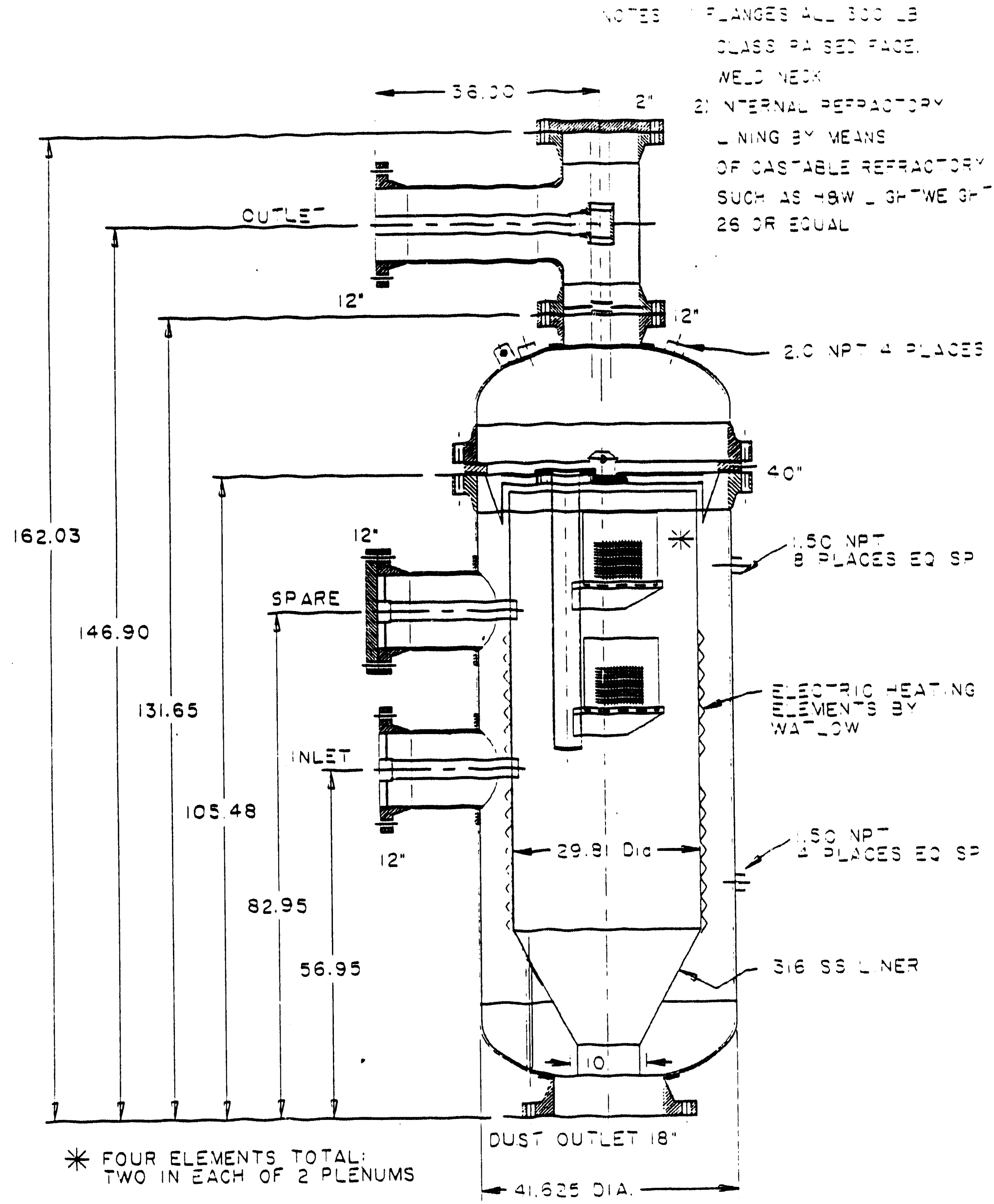

Westinghouse Cross Flow Filter –

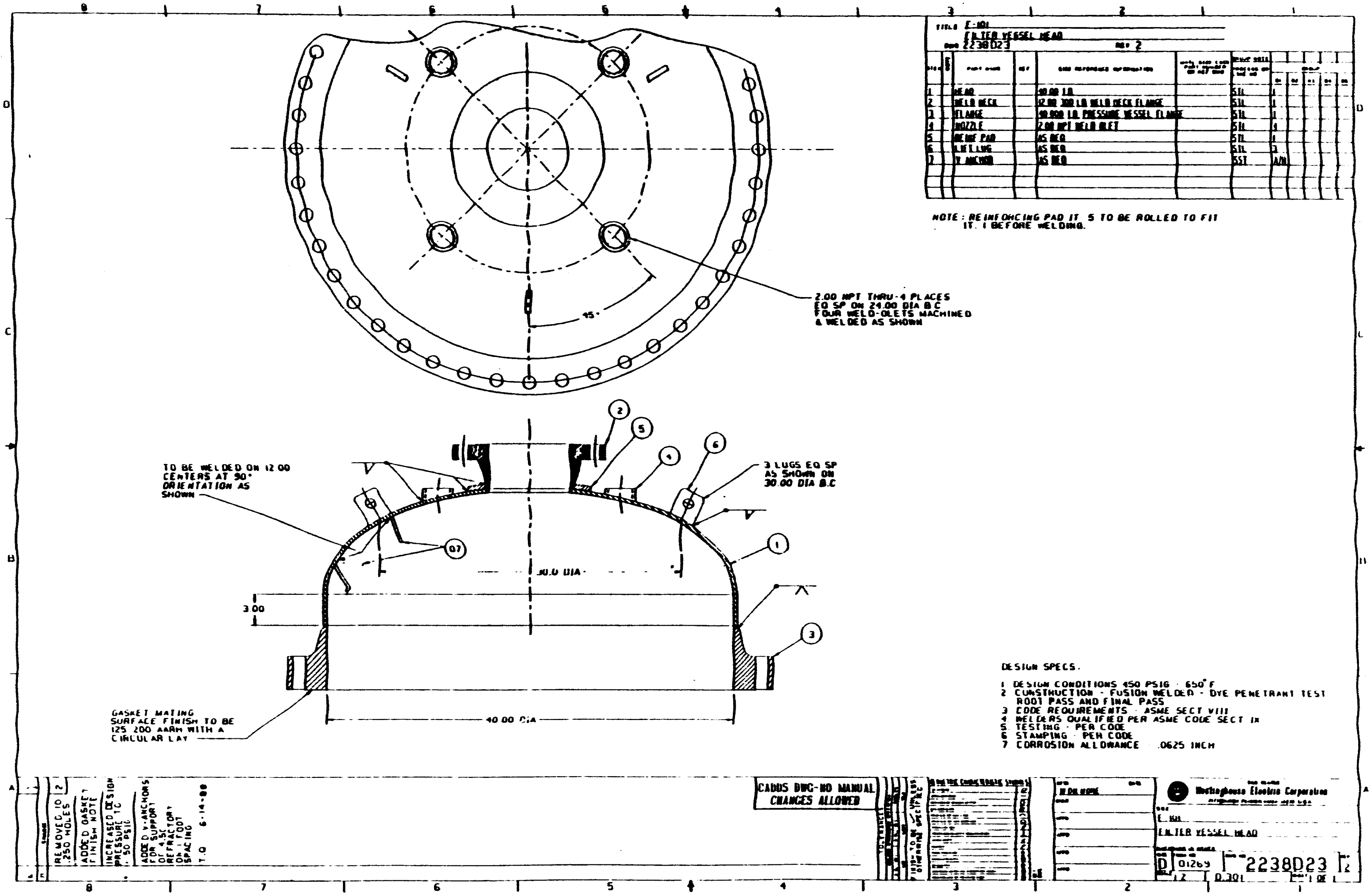
TITLE E-101
FILTER VESSEL HEAD
DWG 2238D23 REV 2
1 HEAD 40.00 I.D. STL 1
2 WELD NECK 12.00 300 LB WELD NECK FLANGE STL 1
3 FLANGE 40.000 LB PRESSURE VESSEL FLANGE STL 1
4 NOZZLE 2.00 NPT WELD OLET STL 4
5 REINF PAD AS REQ STL 1
6 LIFT LUG AS REQ STL 3
7 V ANCHOR AS REQ SST A/R
NOTE: REINFORCING PAD IT. 5 TO BE ROLLED TO FIT IT. 1 BEFORE WELDING.
2.00 NPT THRU-4 PLACES EQ SP ON 24.00 DIA B.C FOUR WELD-OLETS MACHINED & WELDED AS SHOWN
45°
TO BE WELDED ON 12.00 CENTERS AT 90° ORIENTATION AS SHOWN
3 LUGS EQ SP AS SHOWN ON 30.00 DIA B.C
30.0 DIA
3.00
40.00 DIA
GASKET MATING SURFACE FINISH TO BE 125 200 AARH WITH A CIRCULAR LAY
DESIGN SPECS.
1 DESIGN CONDITIONS 450 PSIG · 650°F
2 CONSTRUCTION · FUSION WELDED · DYE PENETRANT TEST ROOT PASS AND FINAL PASS
3 CODE REQUIREMENTS · ASME SECT VIII
4 WELDERS QUALIFIED PER ASME CODE SECT IX
5 TESTING · PER CODE
6 STAMPING · PER CODE
7 CORROSION ALLOWANCE .0625 INCH
2 REMOVED 10 .250 HOLES
ADDED GASKET FINISH NOTE
INCREASED DESIGN PRESSURE TO 450 PSIG
ADDED V-ANCHORS FOR SUPPORT OF 4.5" REFRACTORY ON 1 FOOT SPACING
T.O 6-14-88
CADDS DWG-NO MANUAL CHANGES ALLOWED
Westinghouse Electric Corporation
E-101
FILTER VESSEL HEAD
D 01269 2238D23 2
1/2 0.301 1 OF 1

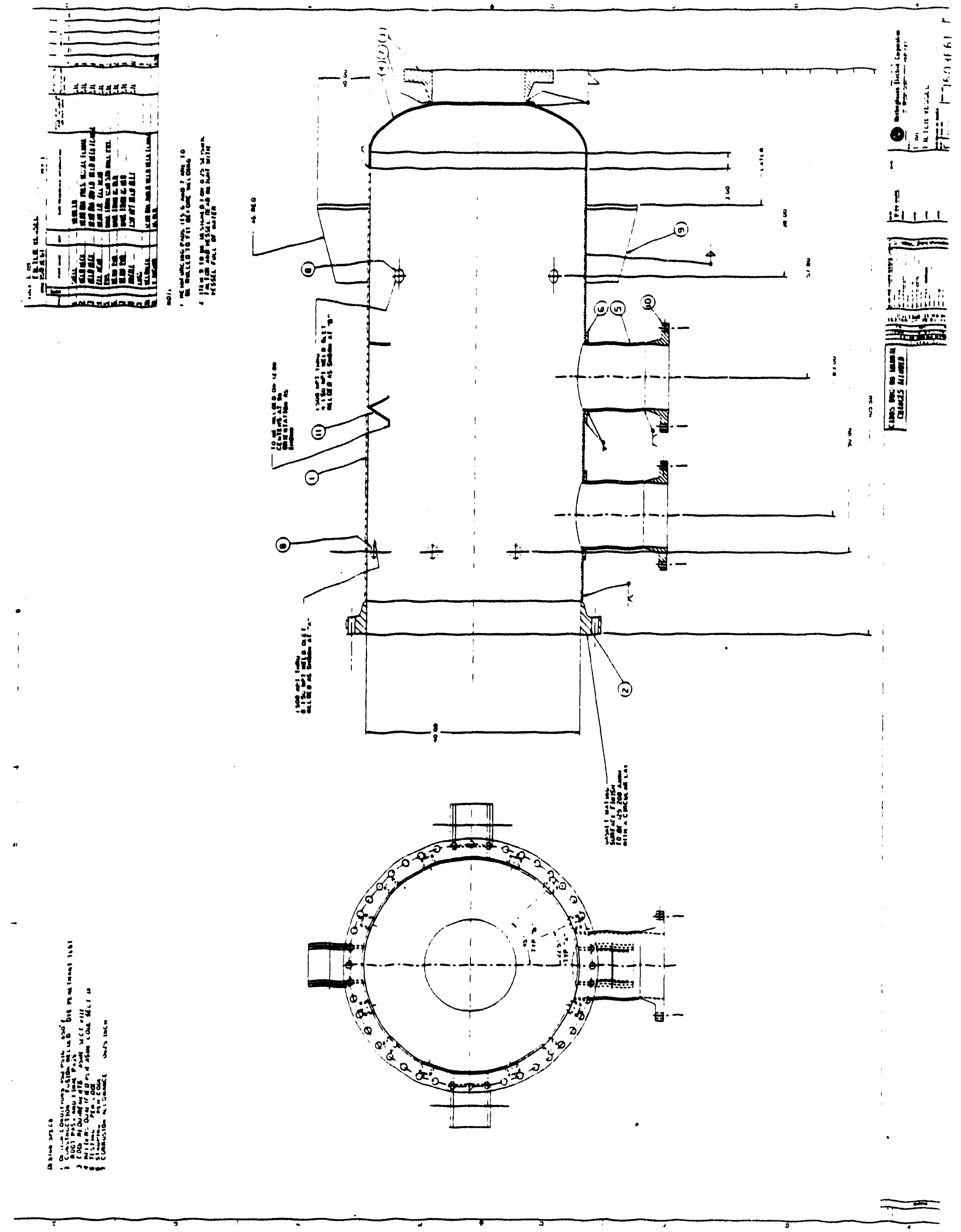

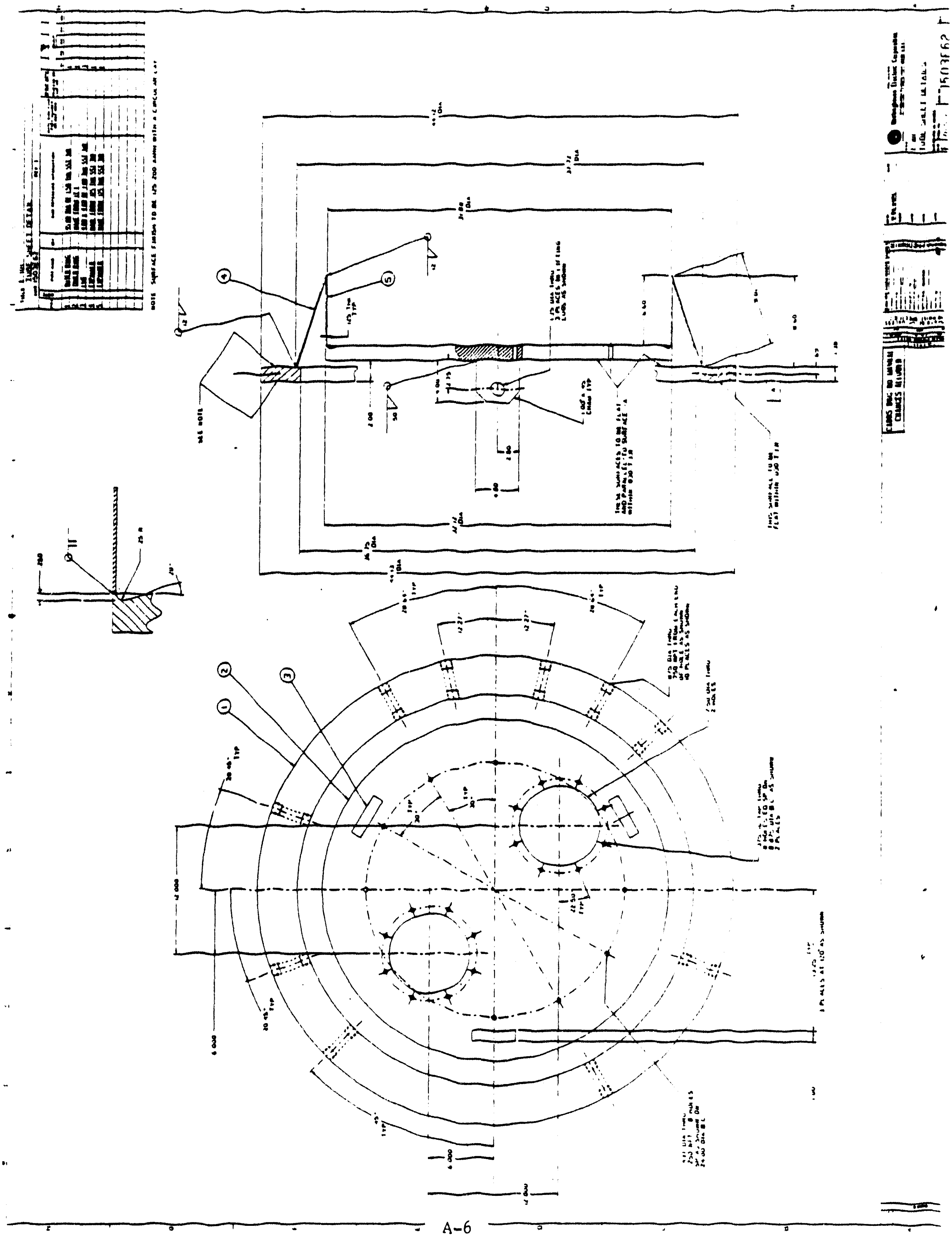

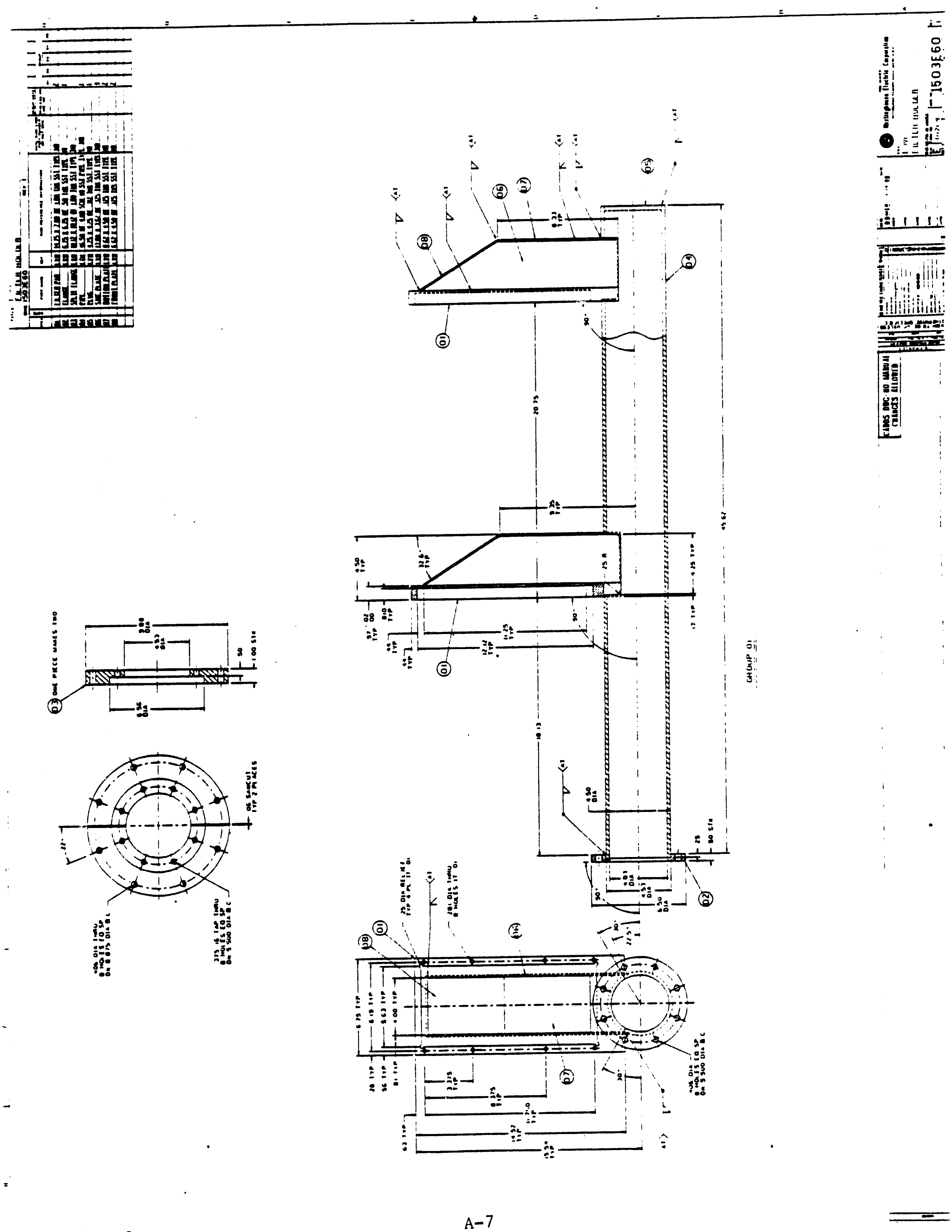
CADDS DWG: NO MANUAL CHANGES ALLOWED
1503E60

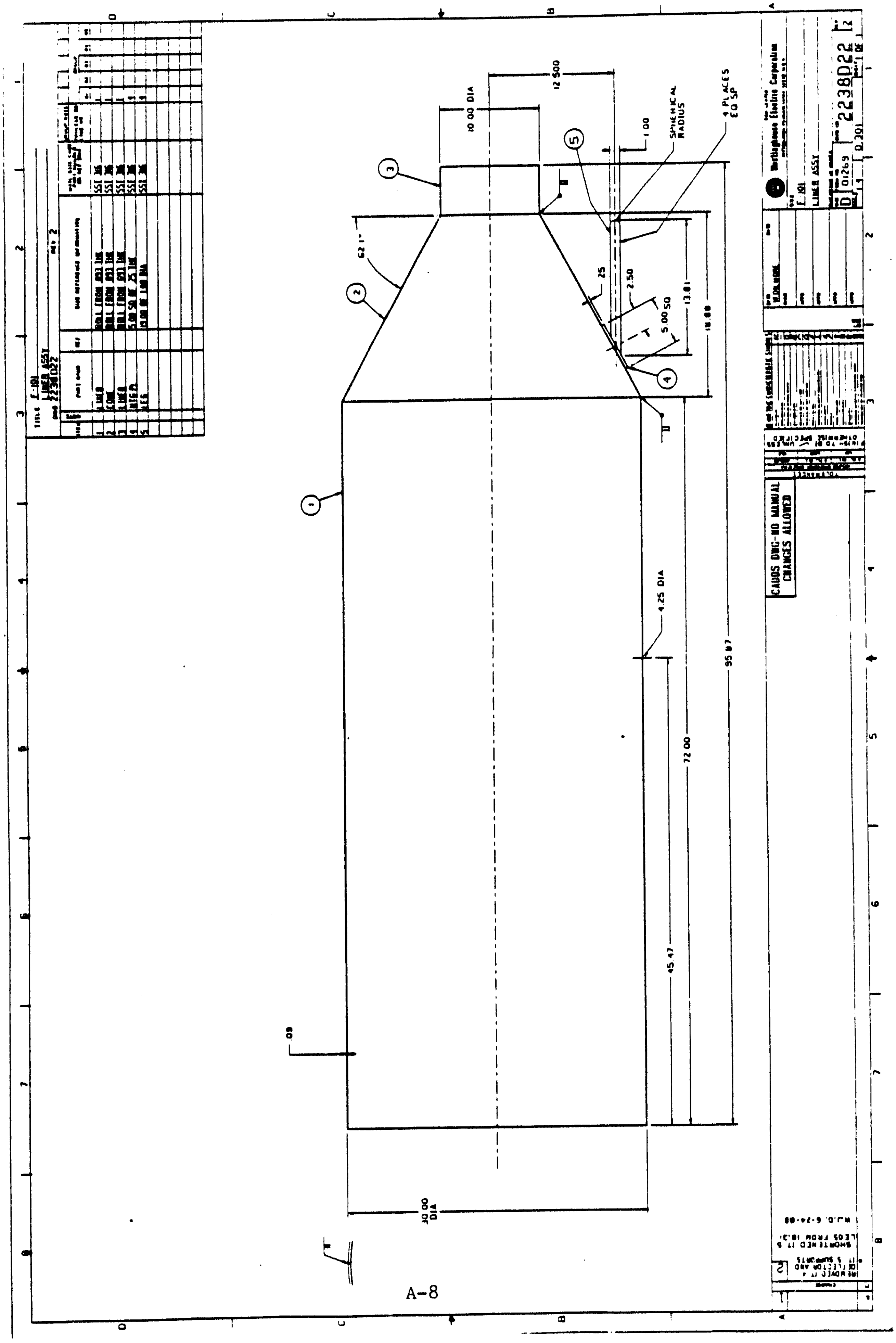

F-101
LINER ASSY
2238D22
REV 2
1 LINER ROLL FROM .093 THK SST 316
2 CONE ROLL FROM .093 THK SST 316
3 LINER ROLL FROM .093 THK SST 316
4 MTG PL 5.00 SQ OF .25 THK SST 316
5 LEG SST 316
10.00 DIA
12.500
1.00
SPHERICAL RADIUS
4 PLACES EQ SP
62.1°
.25
2.50
5.00 SQ
13.81
18.88
4.25 DIA
95.87
72.00
45.47
.09
30.00 DIA
CADDS DWG-NO MANUAL CHANGES ALLOWED
Westinghouse Electric Corporation
F-101
LINER ASSY
2238D22

A-8

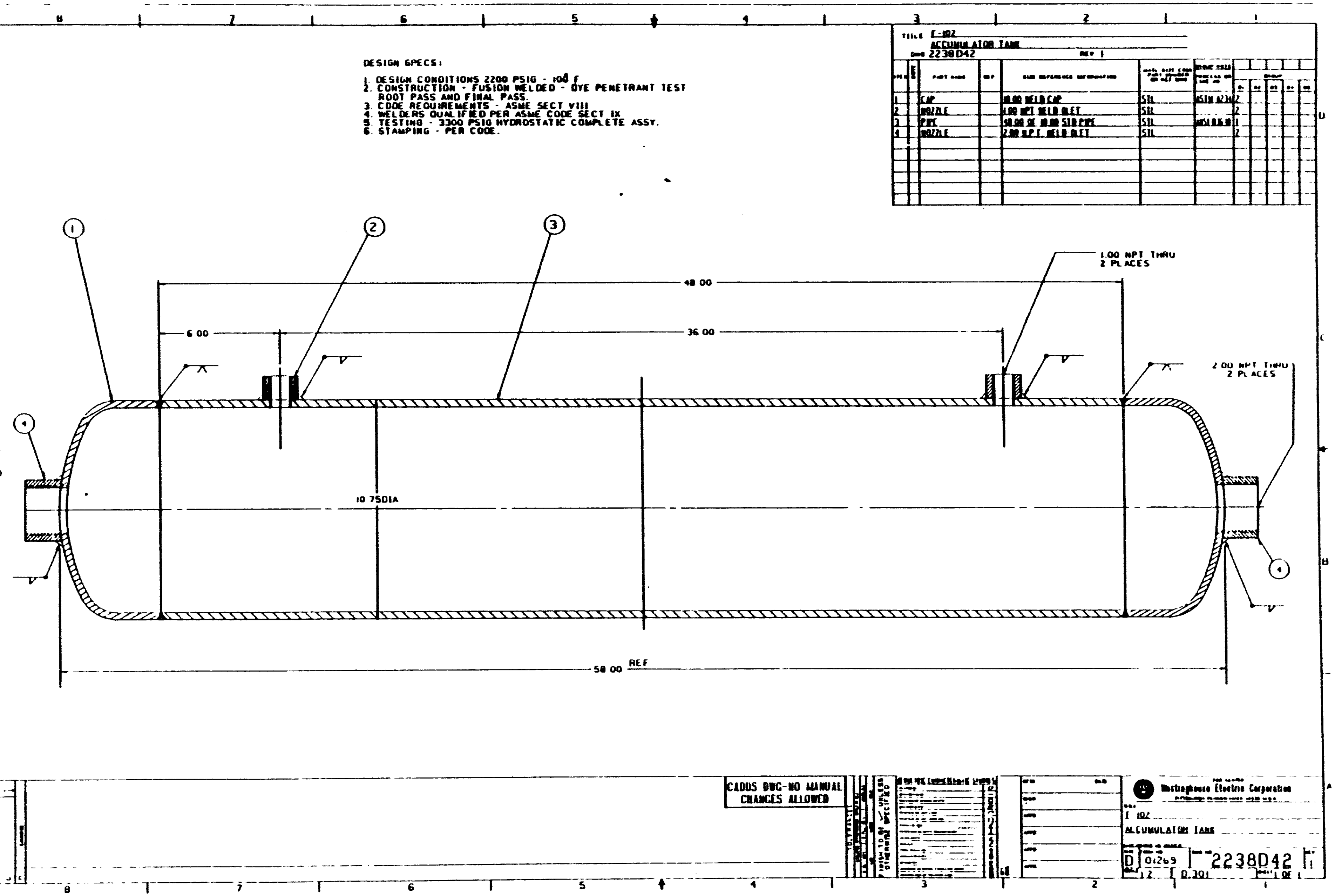
DESIGN SPECS:
1. DESIGN CONDITIONS 2200 PSIG - 100 F
2. CONSTRUCTION - FUSION WELDED - DYE PENETRANT TEST ROOT PASS AND FINAL PASS.
3. CODE REQUIREMENTS - ASME SECT VIII
4. WELDERS QUALIFIED PER ASME CODE SECT IX
5. TESTING - 3300 PSIG HYDROSTATIC COMPLETE ASSY.
6. STAMPING - PER CODE.
TITLE E-102
ACCUMULATOR TANK
DWG 2238D42
REV 1
1 CAP 10.00 WELD CAP STL 2
2 NOZZLE 1.00 NPT WELD OLET STL 2
3 PIPE 48.00 OF 10.00 STD PIPE STL 1
4 NOZZLE 2.00 N.P.T. WELD OLET STL 2
1.00 NPT THRU
2 PLACES
2.00 NPT THRU
2 PLACES
48.00
6.00
36.00
10.750 DIA
58.00 REF
CADDS DWG-NO MANUAL CHANGES ALLOWED
Westinghouse Electric Corporation
E-102
ACCUMULATOR TANK
D 01269 2238D42
1 OF 1

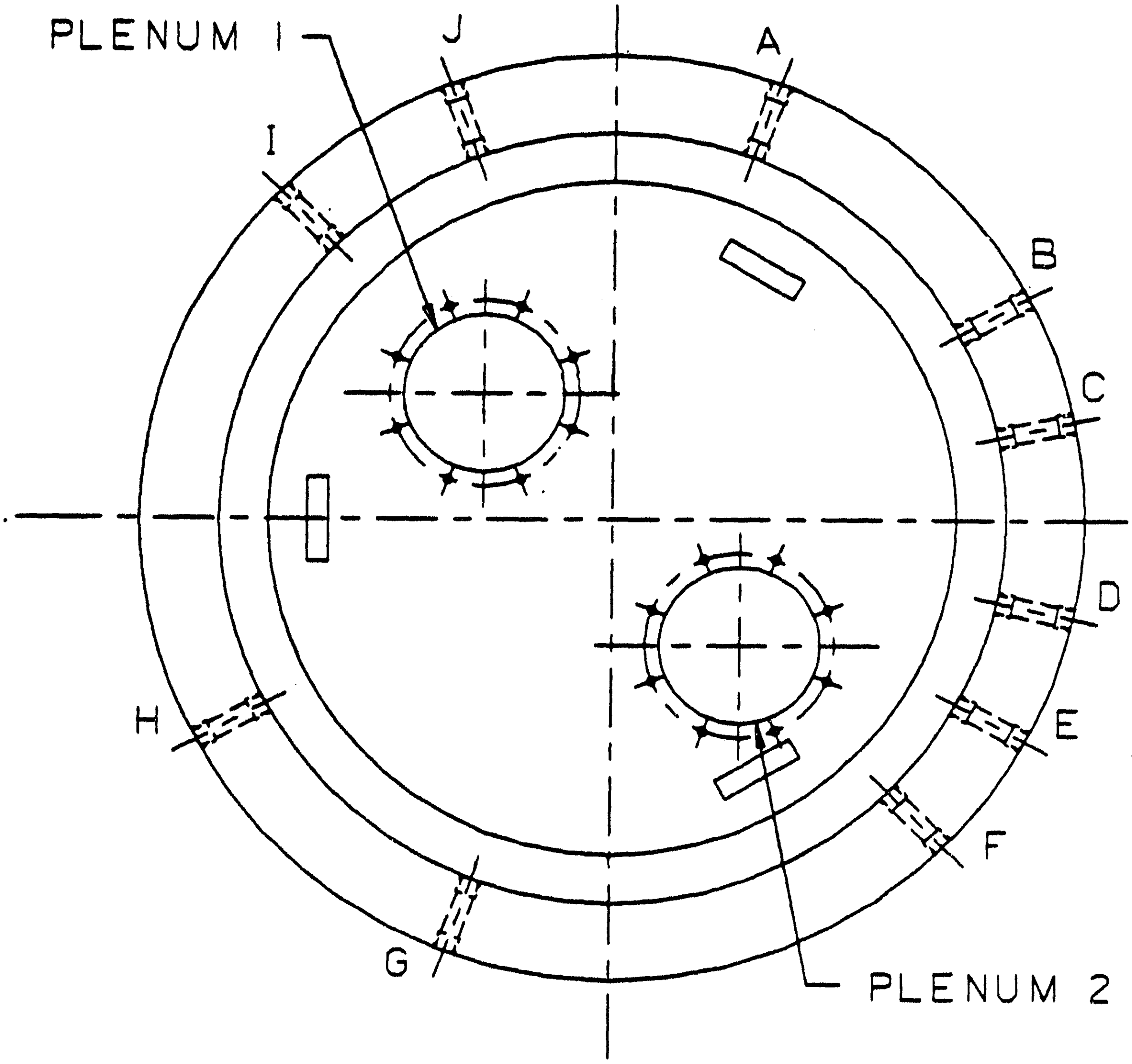

P&ID NO. 1

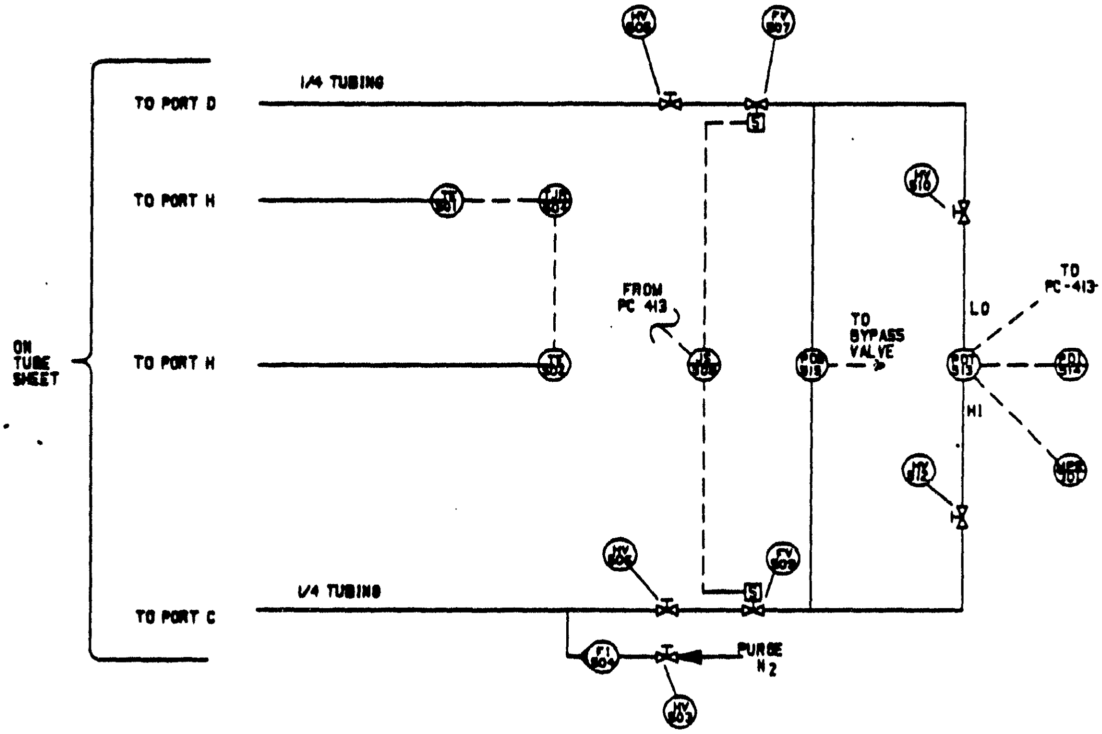

FILTER △ P SYSTEM

P&ID NO. 2

D 301 4134A90.F

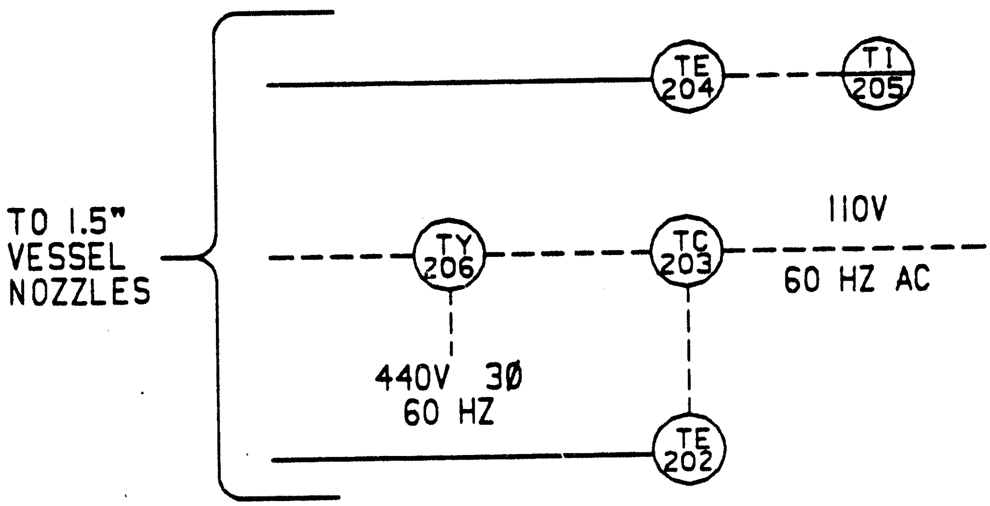

HEATER CONTROL SYSTEM

P&ID NO. 3

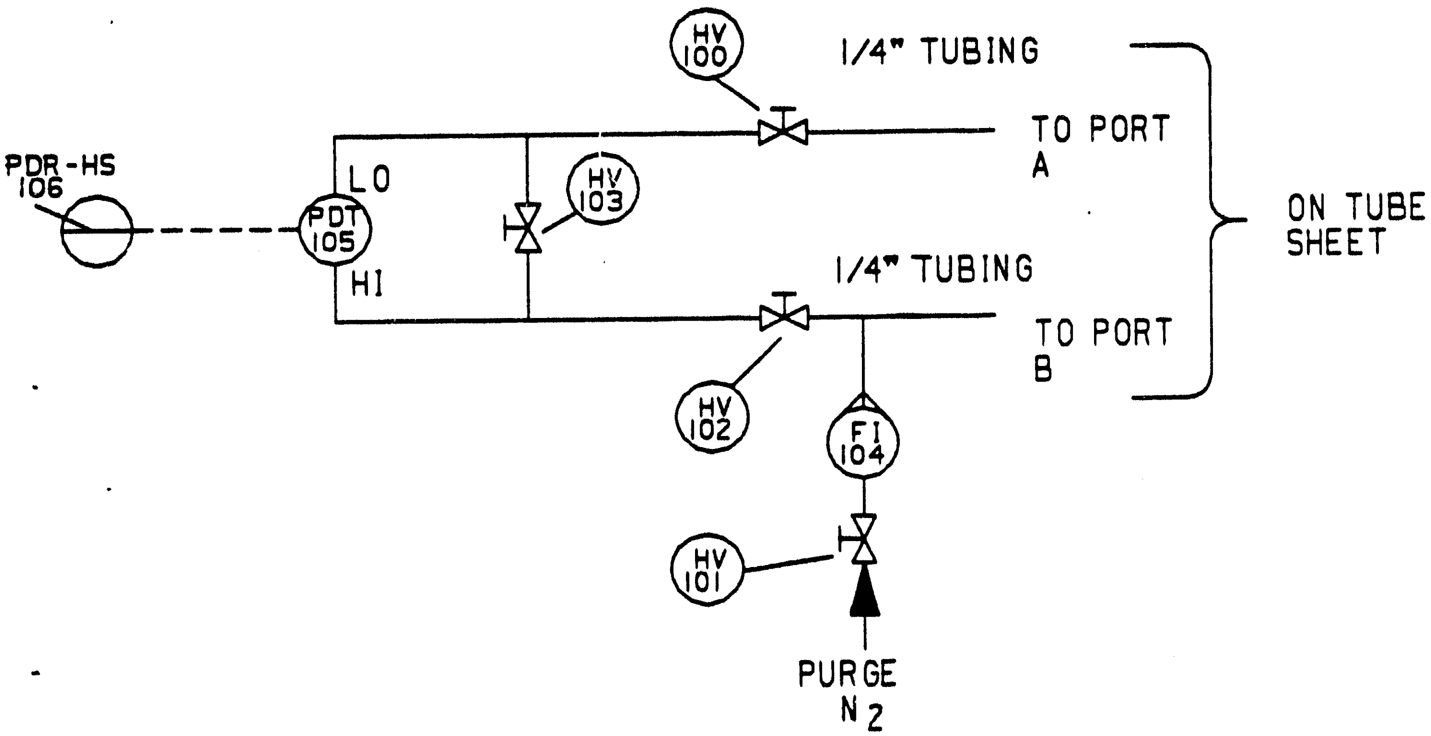

BLOW BACK PULSE PRESURE SYSTEM

P&ID NO. 4

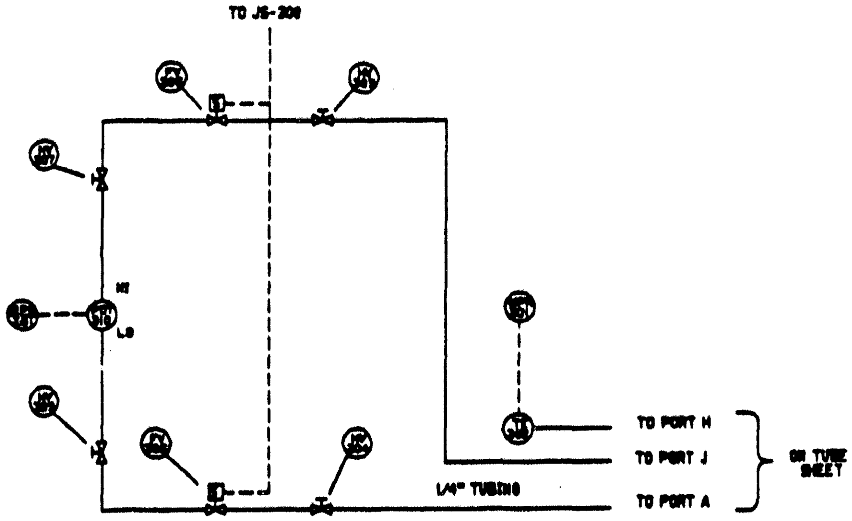

FILTER PLENUM 1 FLOW SYSTEM

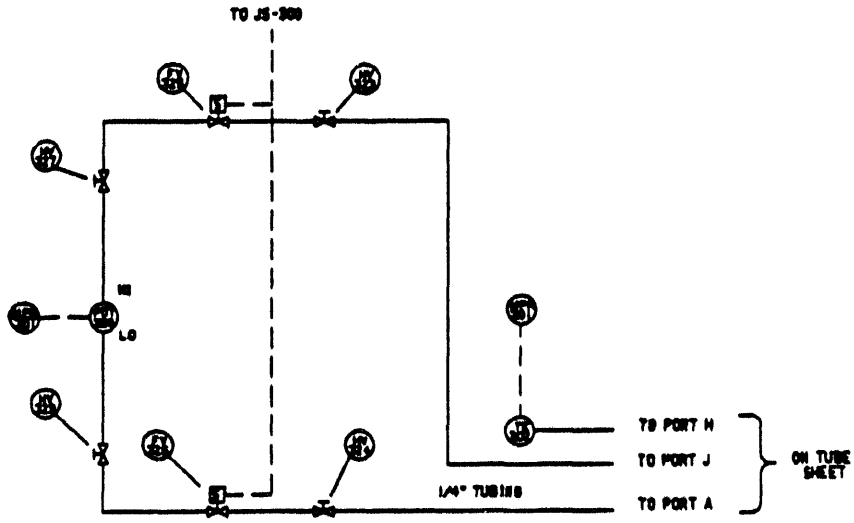

FILTER PLENUM 2 FLOW SYSTEM

P&ID NO.5

D.301.4134A93.R1

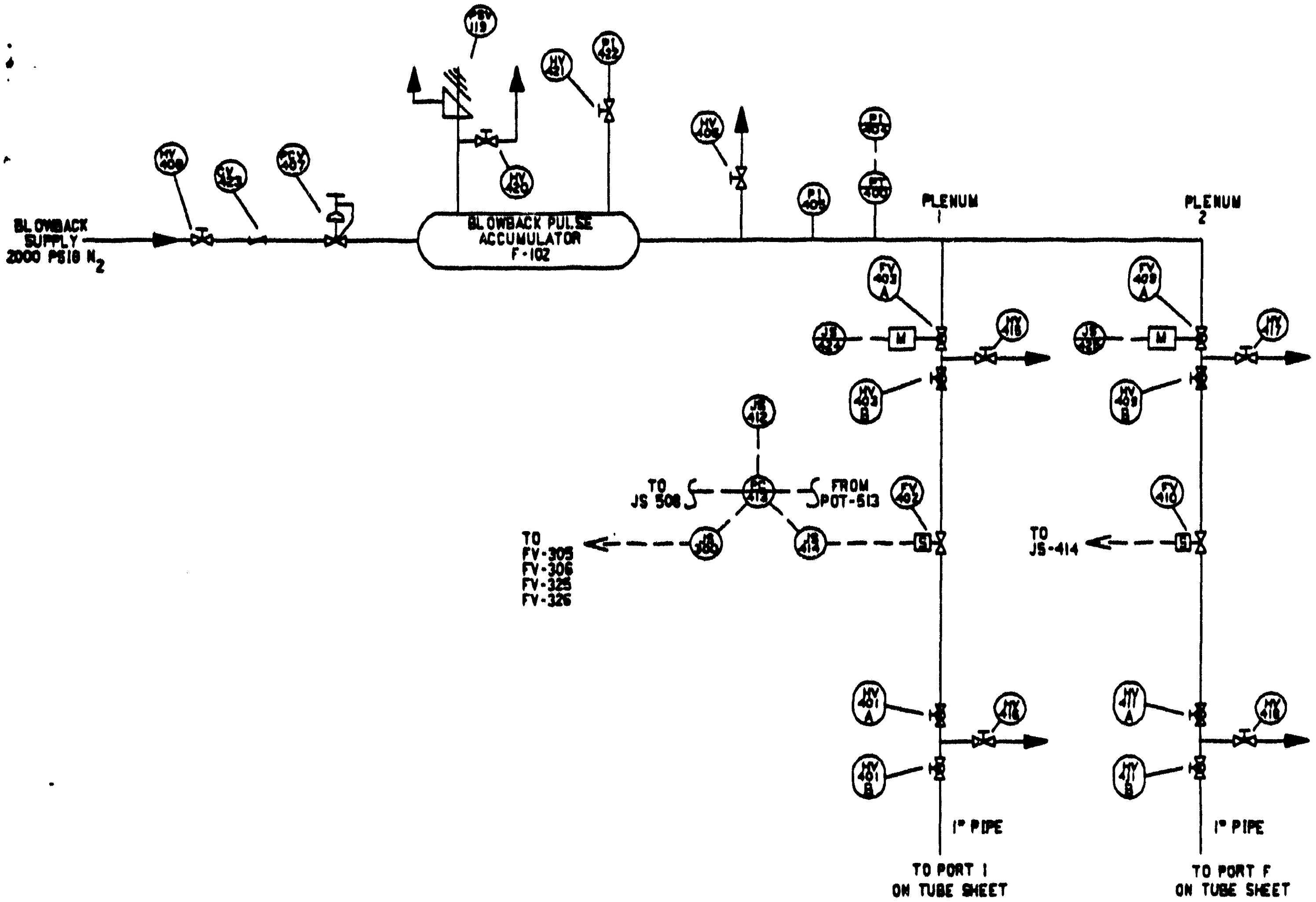

FILTER BLOWBACK SYSTEM

P&ID NO.6

D.301.4134A94.R1

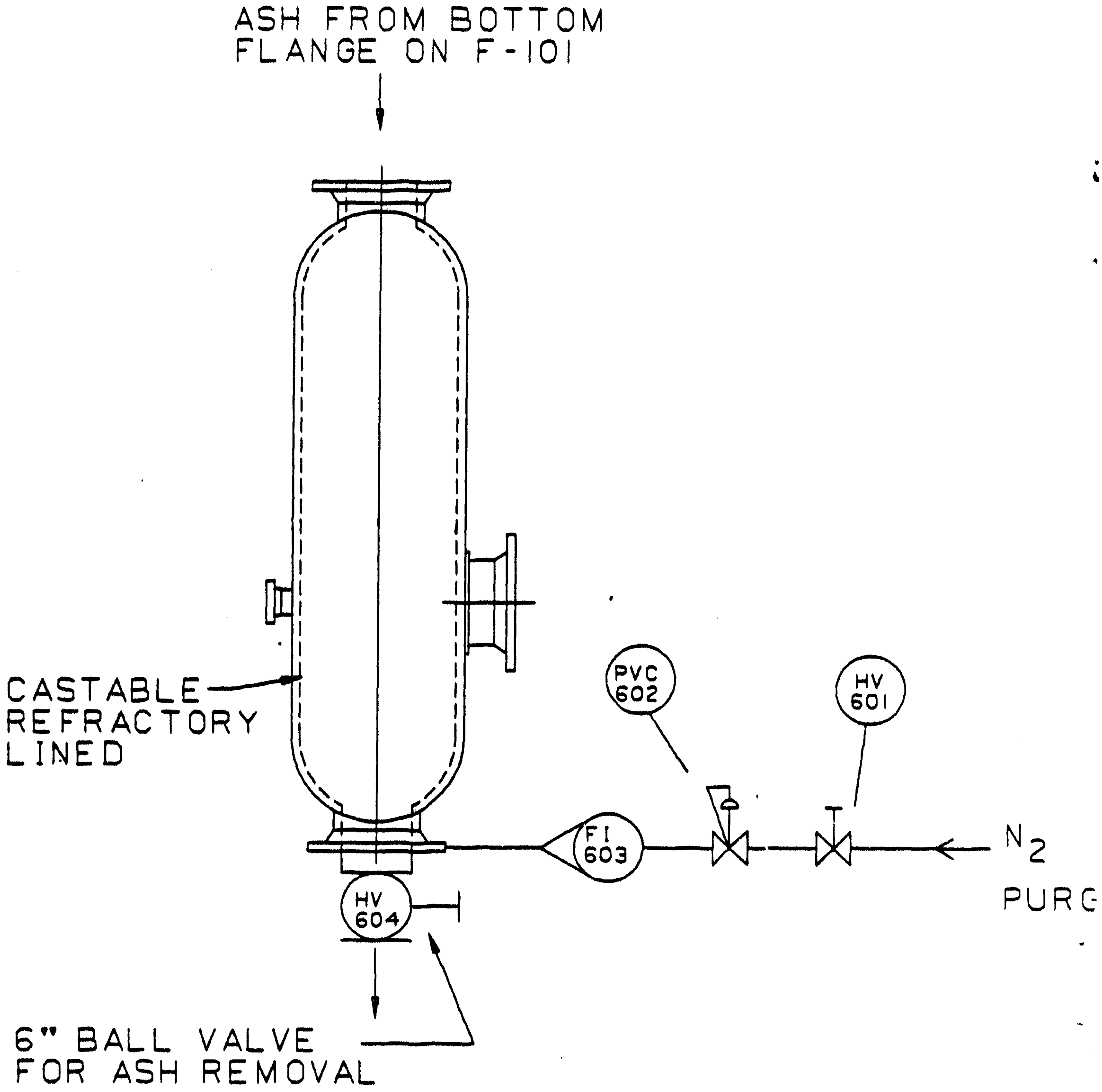

ASH COLLECTION POT F-103

P&ID NO. 7

D.301.4134A95.R1

APPENDIX B

Results of Laboratory Analysis of Filter Catch - April 1989 Test

LABORATORY ANALYSIS OF PARTICULATE SOLIDS
(By Southern Research Institute)

The laboratory tests described in this report were performed on a bulk sample (1 qt) of material identified as sample number 89MRL047. This material was collected in the ash pot, which is attached directly to the bottom of the filter vessel, after the completion of the checkout run of the Westinghouse Ceramic Cross-Flow Filter in April 1989. The test methods and results are described in the following paragraphs, and brief explanations of the significance of the results are given where appropriate.

Bulk Porosity - This value expresses the resultant porosity of a column of material under a given compressive load (including zero for the uncompacted bulk porosity). Relatively large values of bulk porosity correspond to highly cohesive particles. The results for the sample provided were as follows:

Uncompacted bulk porosity - 91.6%
Compacted bulk porosity - 70.7%

The latter measurement is somewhat arbitrary, corresponding to a load near the asymptotic limit of compaction for our specific laboratory apparatus. Furthermore, in the case of very porous materials such as the given sample, the compaction cell will not hold enough material to compare with less porous samples. The values of porosity measured for the sample under test were very large compared with conventional fly ashes and similar materials. Gasifier chars taken downstream of recycle cyclones are even more porous, however.

Density - Determination of the true particle density is a standard measurement that is made with a helium pycnometer. The particle density is required for calculating dust cake and bulk porosities. It is also used in developing the relationship between the dust cake thickness and the areal density for a given material. The true particle density for the sample is 2.62 g/cm^3.

Particle Size Distribution - Our usual laboratory procedure employs the Bahco classifier to determine the particle size distribution in terms of aerodynamic diameters. This sample did not behave well in the Bahco device; there was a strong tendency to clog the feed nozzle. Only the first two cut points could be determined with any reliability at all. These results showed 7.8% of the mass was less than 1.5 μmin diameter, and 14.6% was smaller than 2.3 μm.

Relative gas flow resistance - This test is performed by filtering air at a measured flow rate through a simulated dust cake of know porosity in a laboratory device, while measuring the pressure drop. The simulated dust cake is free of cracks and crevices, and its porosity is uniform and homogeneous. In this test the relative gas flow resistance was found to be 1.0 in H_2O•min•fit/lb at an estimated porosity of 91.6%. This value is low compared with the relative gas flow resistances of most fly ashes from pulverized coal boilers and AFBC plants.

Drag-equivalent Diameter - This quantity is not a measurement of a physical dimension, but a fitted parameter ranking the characteristic gas flow resistances of particulate materials at equivalent dust cake porosities. Increasing values of drag-equivalent diameters indicate lower resistance to gas flow at a given porosity. Measurements of physical size generally correlate with this expression; however, the drag-equivalent diameter best expresses the fineness of an ash as it relates to its effect on relative gas flow resistance. Determining the value of this quantity is a way to take into account the implicit effects of such characteristics as morphology and cohesivity of the material. The drag-equivalent diameter for the test material was 0.621 μm which is quite small compared with the values of this quantity for PC, AFBC, and CFBC ashes. The relatively low gas flow resistance arises from the compensating effect of the high degree of porosity.

Scanning Electron Microscopy - A series of SEM photographs were taken and evaluated. At the lowest magnification, many particles have dimensions of 100 μm or more. That results is not surprising, given the nature of the process and the absence of any kind of collecting device upstream of the filter system. It is not necessarily true that the largest of these particles actually reached the dust cake; gravitational settling may have removed some of them as they entered the enclosure.

At higher magnification, the intermediately sized particles are nearly spherical in shape, with relatively smooth surfaces. Most of the particles, however, have a rough spongy-looking texture. The combination of fairly smooth, spherical particles and rough, irregularly shaped particles is an unusual combination.

The highest magnification showed the presence of many sub-micron particles. They show up especially well on the relatively smooth surfaces of the spherical particles. It would be difficult to see them at all on the rougher particles.

Clearly, a large fraction of the mass could be removed by the use of a mechanical collector upstream of the filter system, since there are substantial numbers of particles larger than 20-50 μm. The sub-micron particles might cause problems with pressure drop, but there will probably be enough particles of intermediate size to moderate any unfavorable effects.

APPENDIX C

Filter Pressure Drop Characteristics During Operation on the Texaco Entrained Gasifier

Test Run 6 - Cross Flow Filter
Test Run 10 - Candle Filter

Test Run 6 - Cross Flow Filter Pressure Drop Data

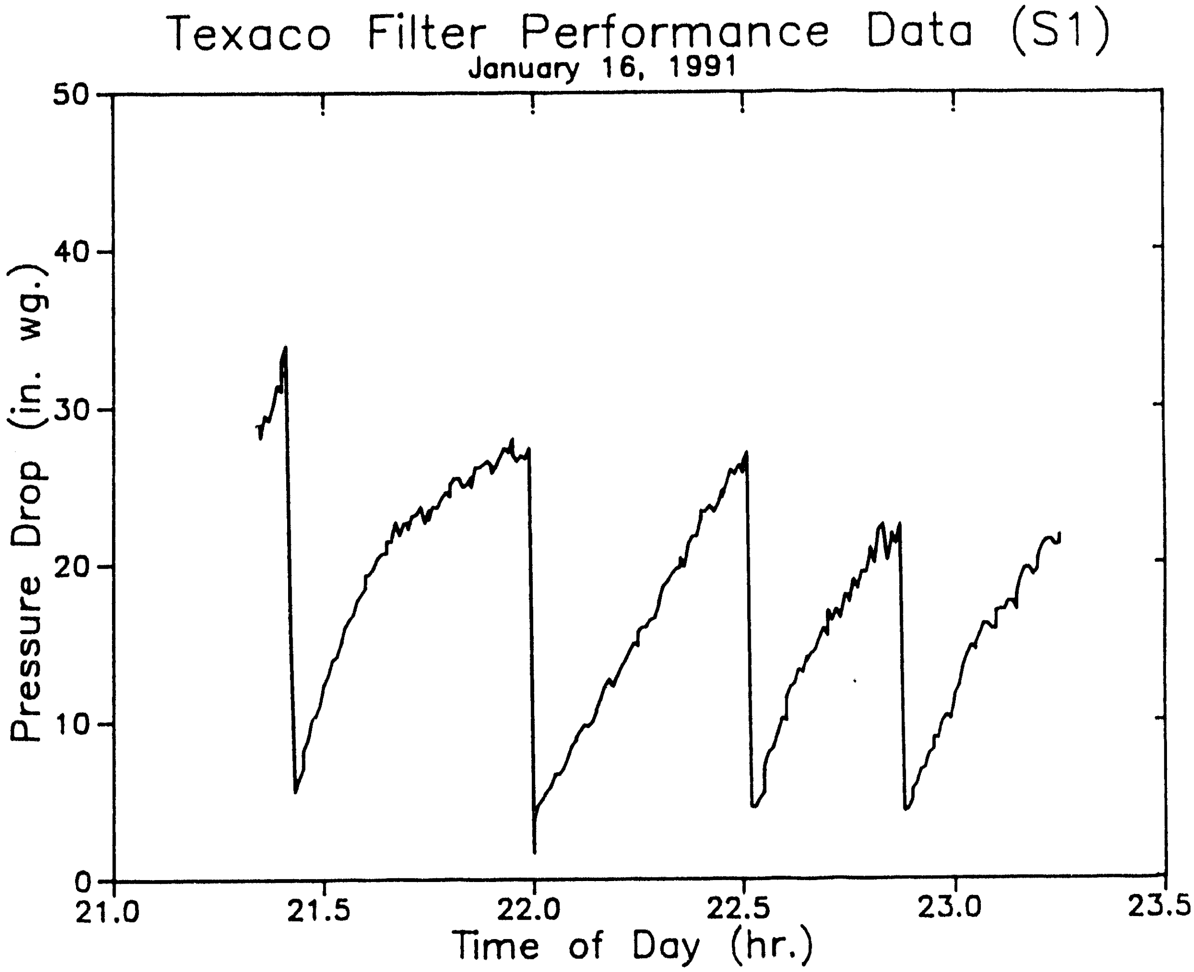
Texaco Filter Performance Data (S1)
January 16, 1991
Pressure Drop (in. wg.)
0
10
20
30
40
50
21.0
21.5
22.0
22.5
23.0
23.5
Time of Day (hr.)

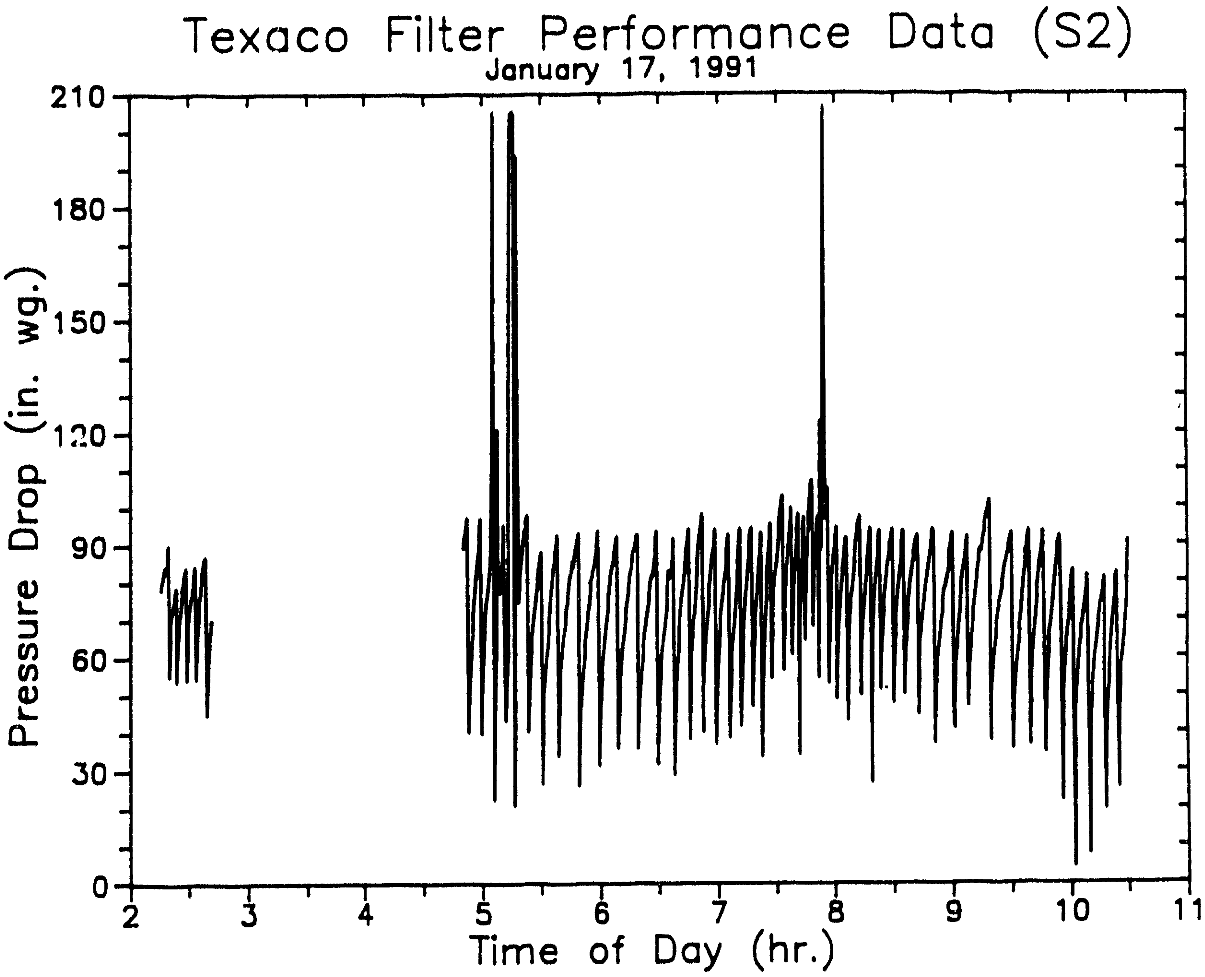

Data between 02:42 and 04:50 missing due to communications interruption
05:11 delta–P line clogged – blown out
07:48 delta–P line clogged – blown out

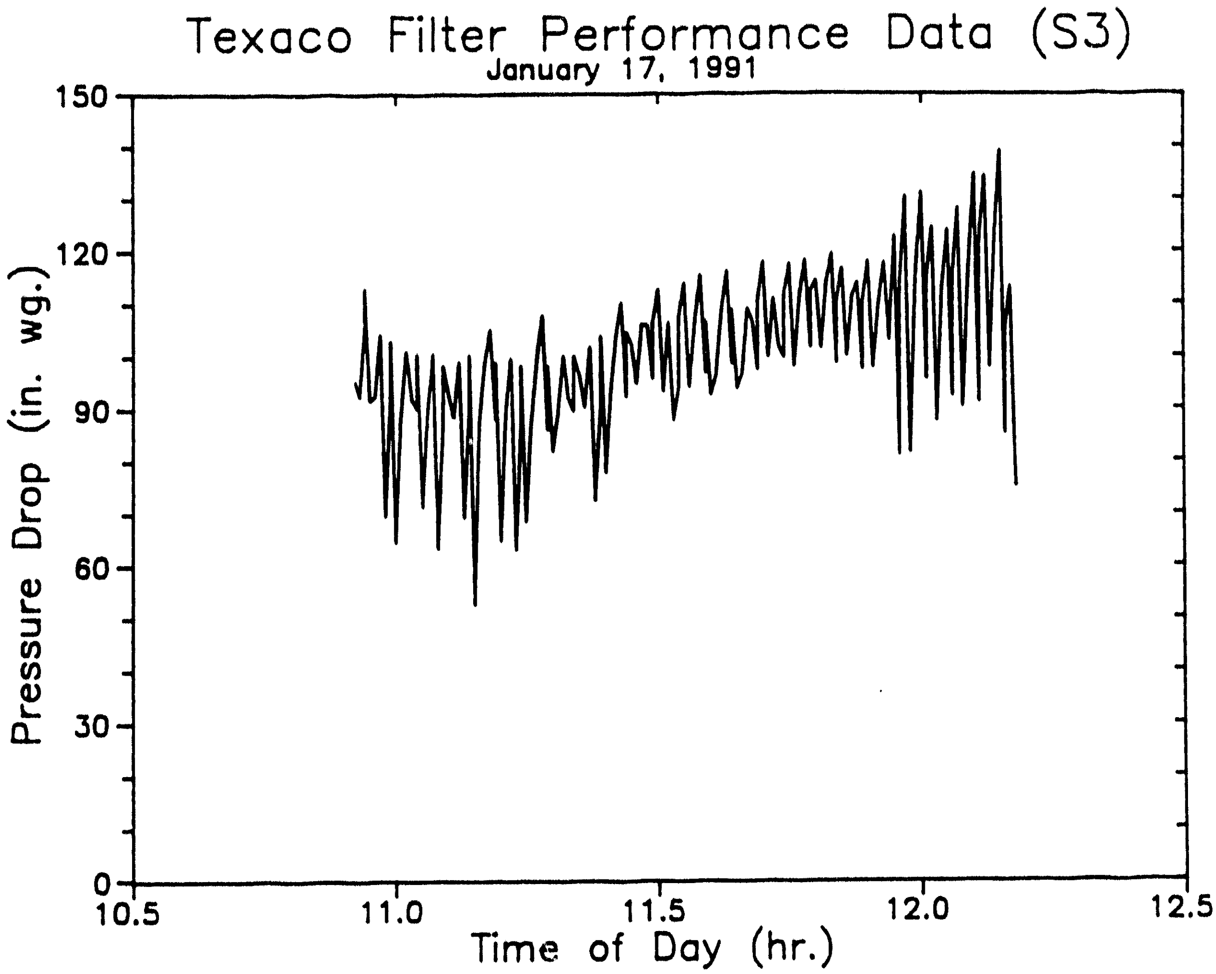

Texaco Filter Performance Data (S3)
January 17, 1991
150
120
90
60
30
0
10.5
11.0
11.5
12.0
12.5
Pressure Drop (in. wg.)
Time of Day (hr.)

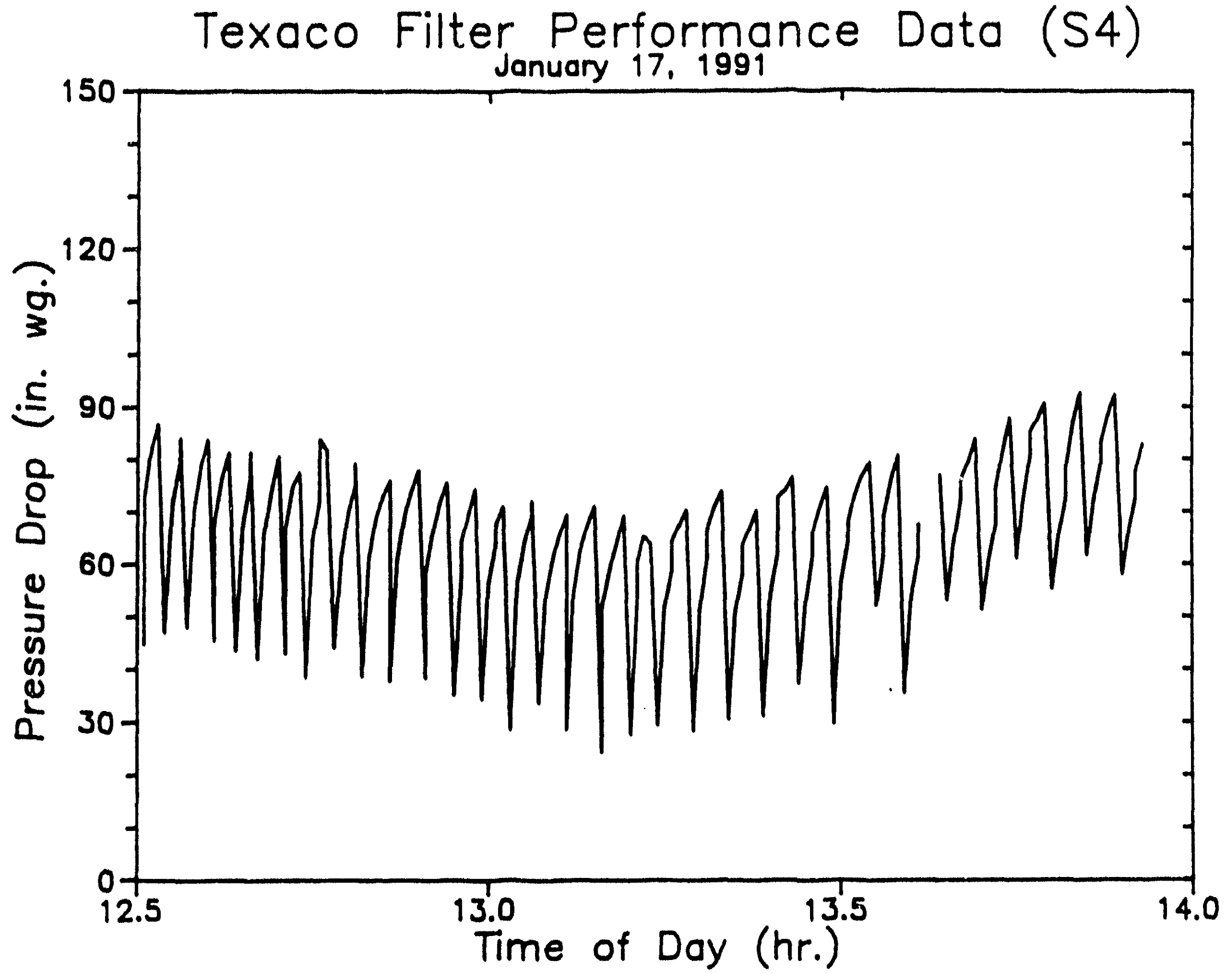
Texaco Filter Performance Data (S4)
January 17, 1991
Pressure Drop (in. wg.)
150
120
90
60
30
0
12.5
13.0
13.5
14.0
Time of Day (hr.)

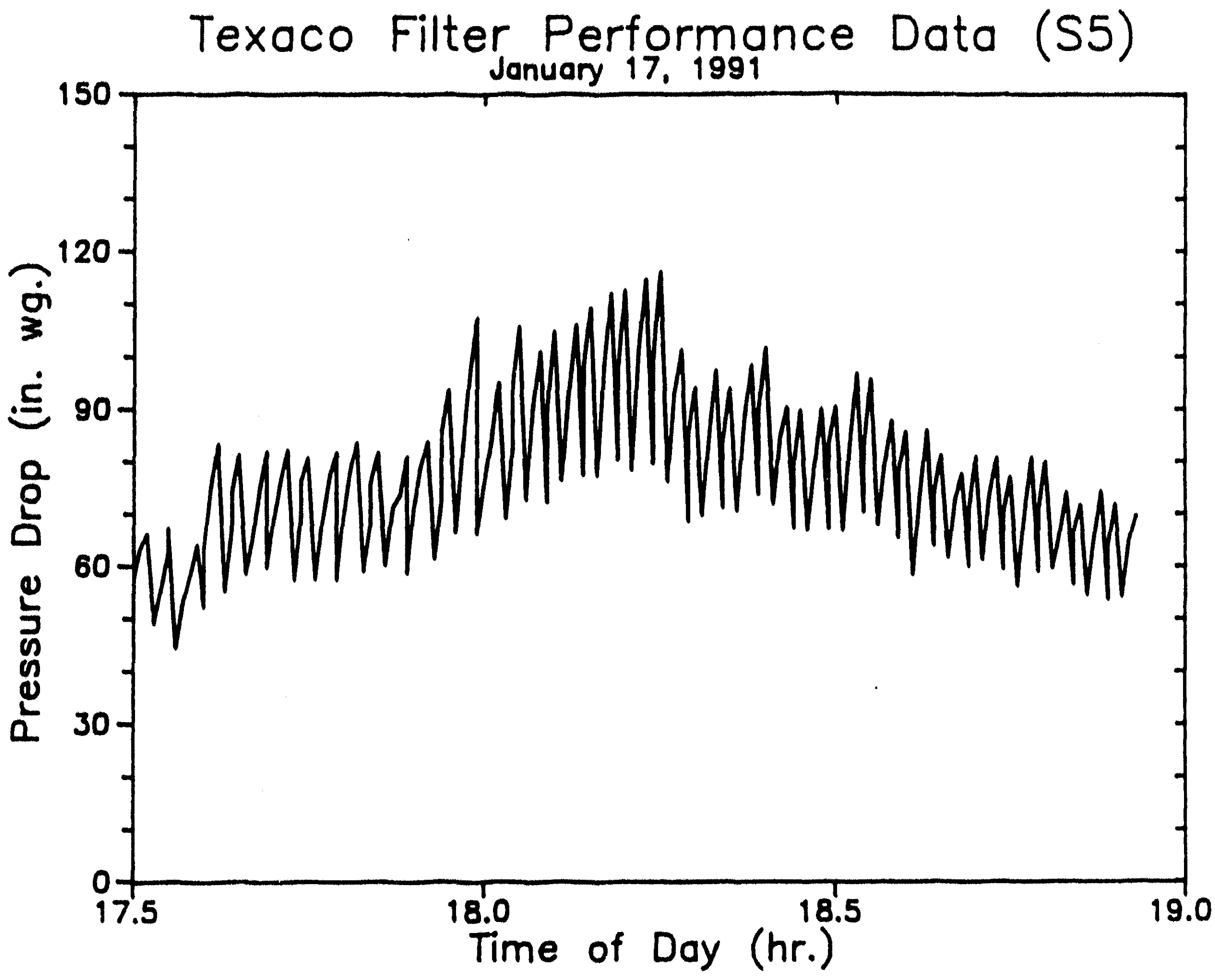
Texaco Filter Performance Data (S5)
January 17, 1991
150
120
90
60
30
0
17.5
18.0
18.5
19.0
Pressure Drop (in. wg.)
Time of Day (hr.)

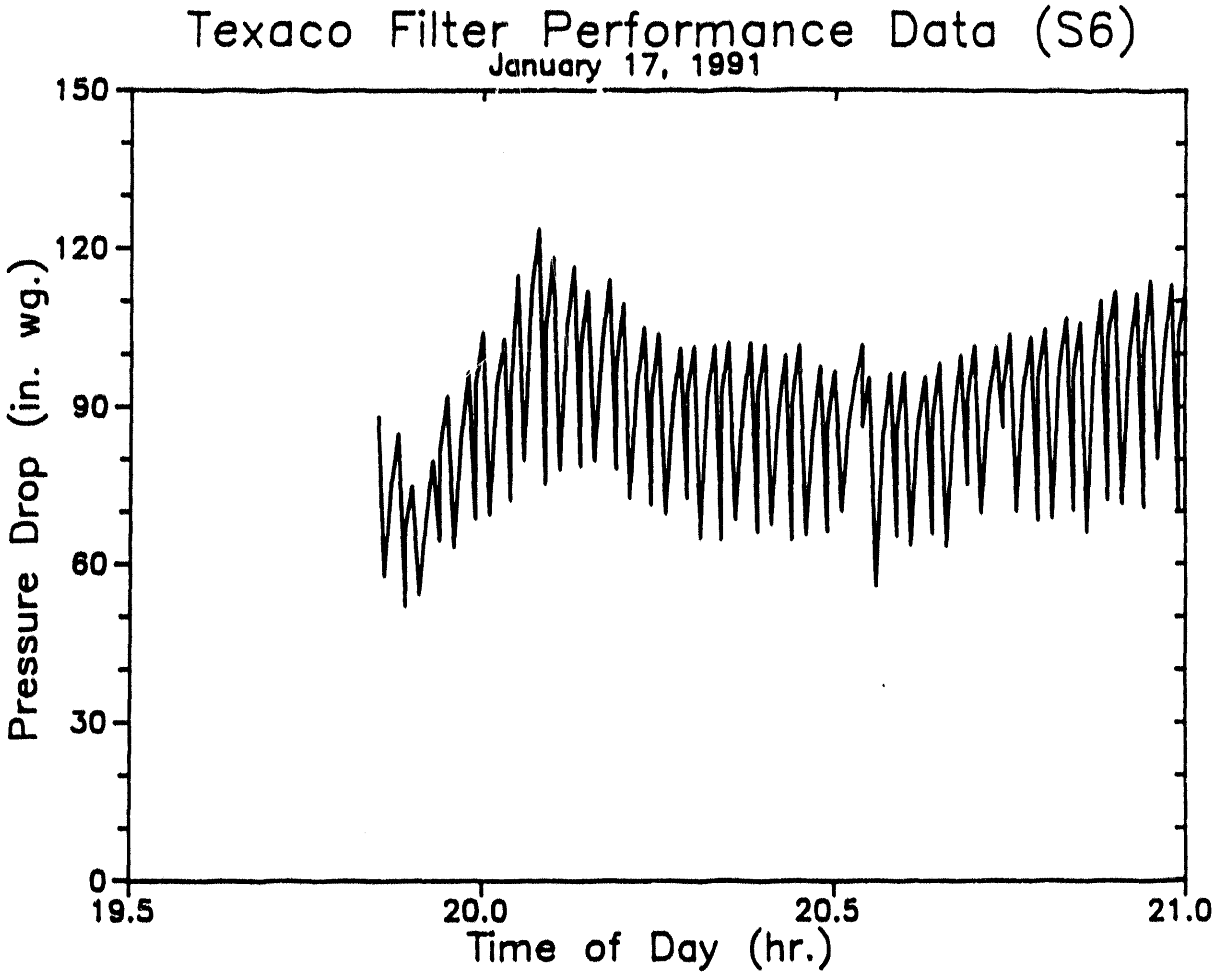

Texaco Filter Performance Data (S6)
January 17, 1991
150
120
90
60
30
0
Pressure Drop (in. wg.)
19.5
20.0
20.5
21.0
Time of Day (hr.)

Figure 14

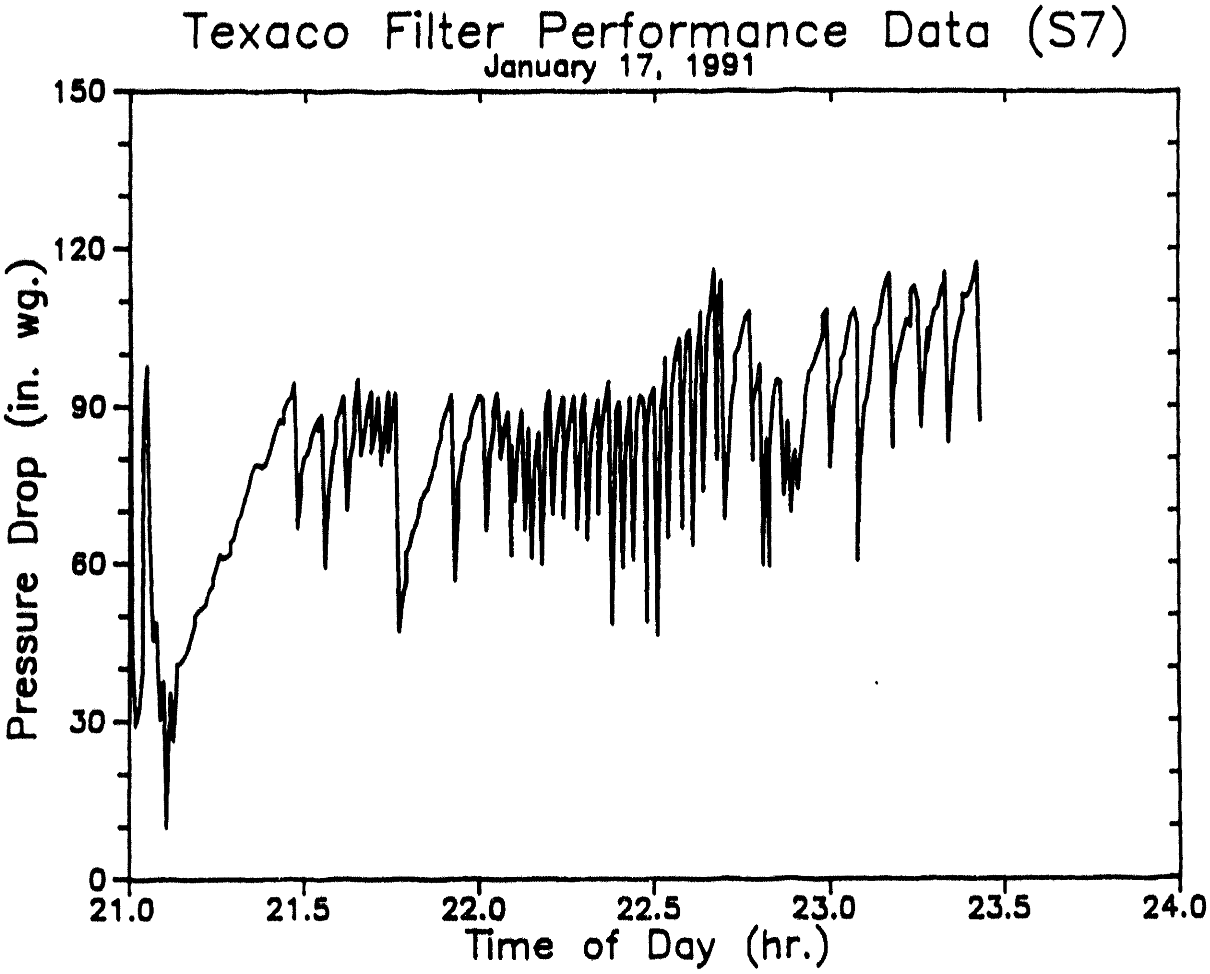

21:05 open By-Pass - 26 in.
21:30 Pulsing P1 only
21:44 Pulsing P2 only
22:30 delta-P lines purged
22:40 Pulsing both plenums
23:03 open By-pass - 33 in.
23:52 disble P2

Test Run 10 - Candle Filter
Pressure Drop Data

Figure 1

Texaco Filter Performance Data

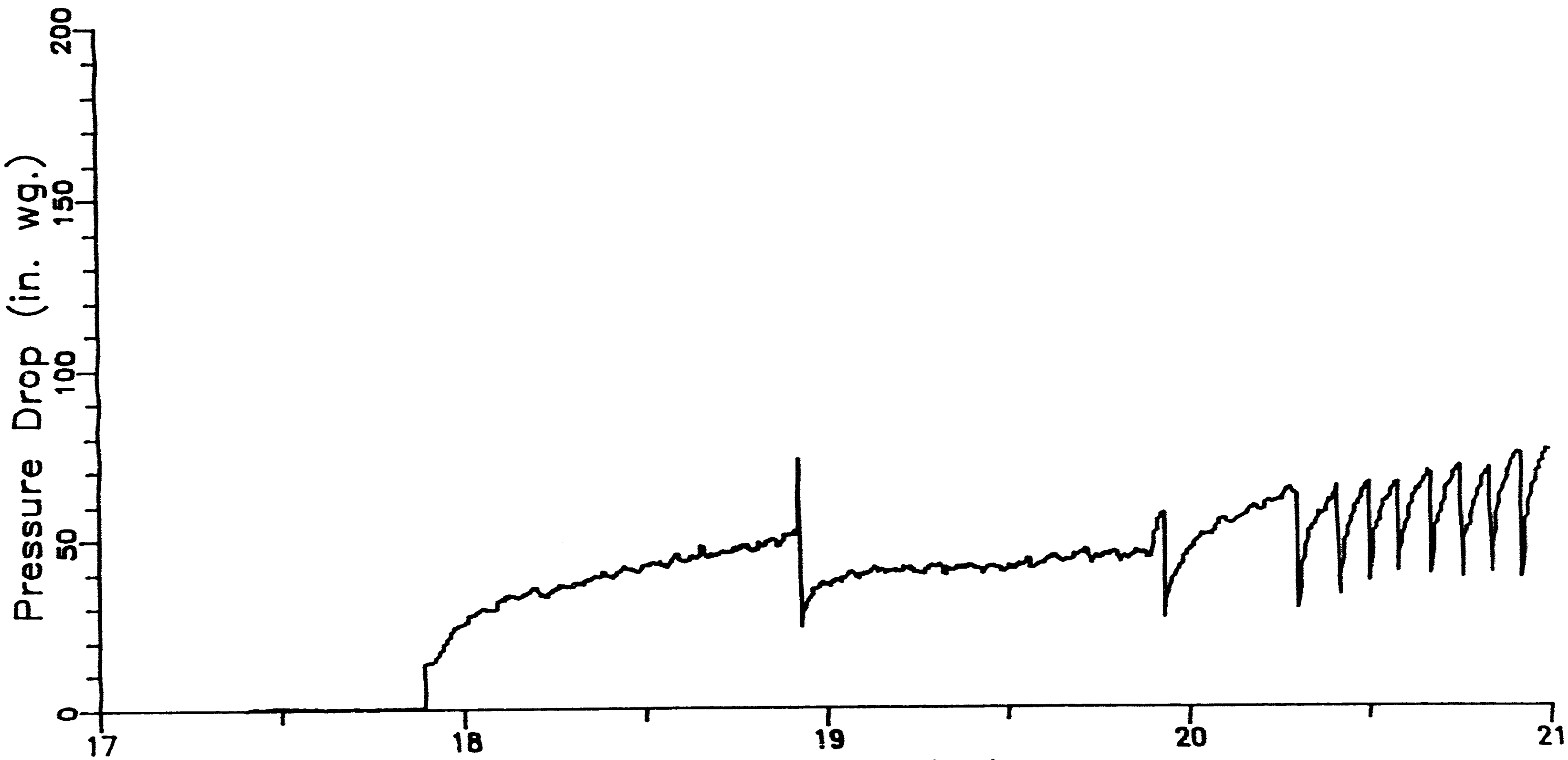

December 4, 1991

1516 Startup (Light-off)

1726 Flow started to filter system

Figure 2

Texaco Filter Performance Data

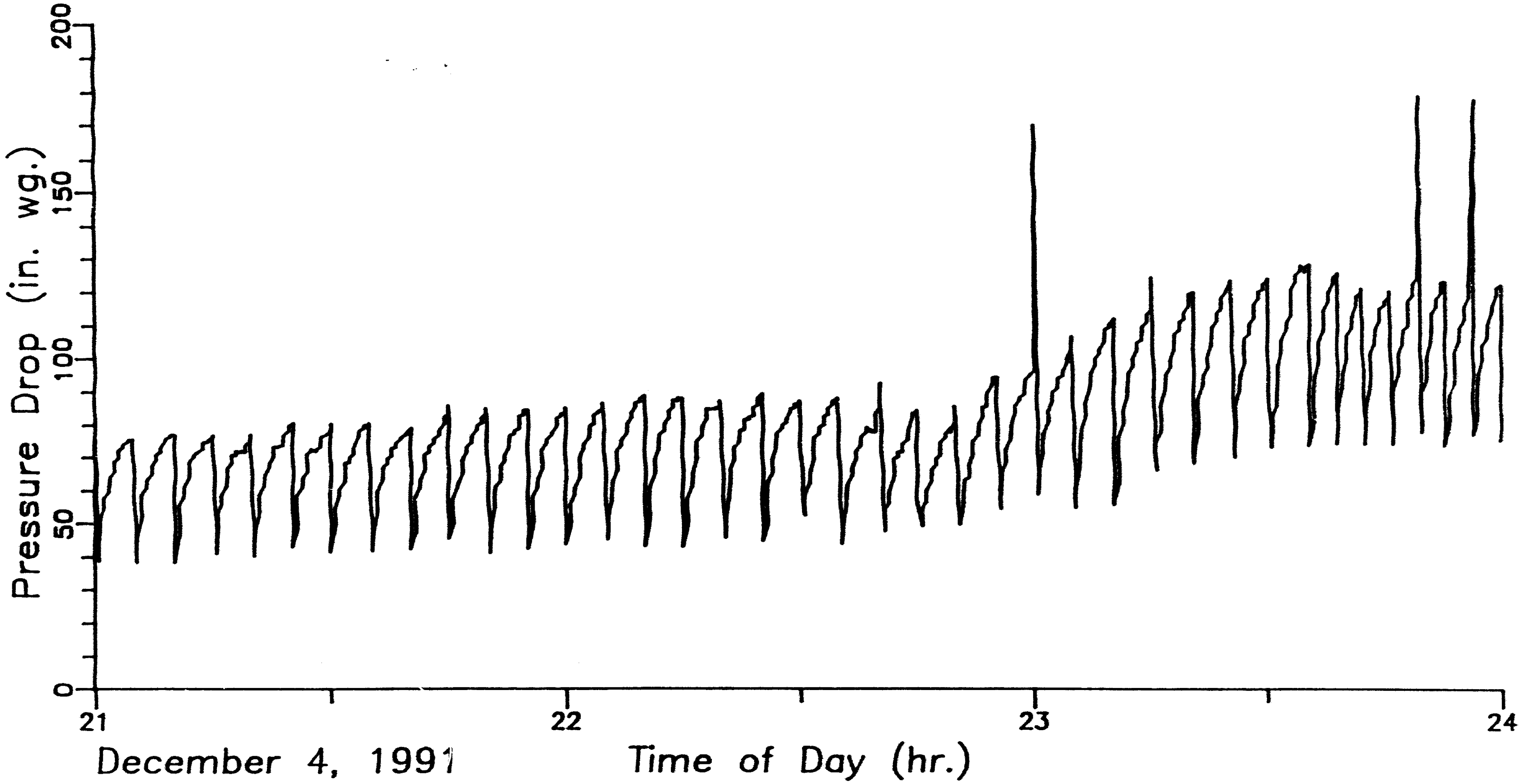

December 4, 1991

2252 Flow increase

Figure 3

Texaco Filter Performance Data

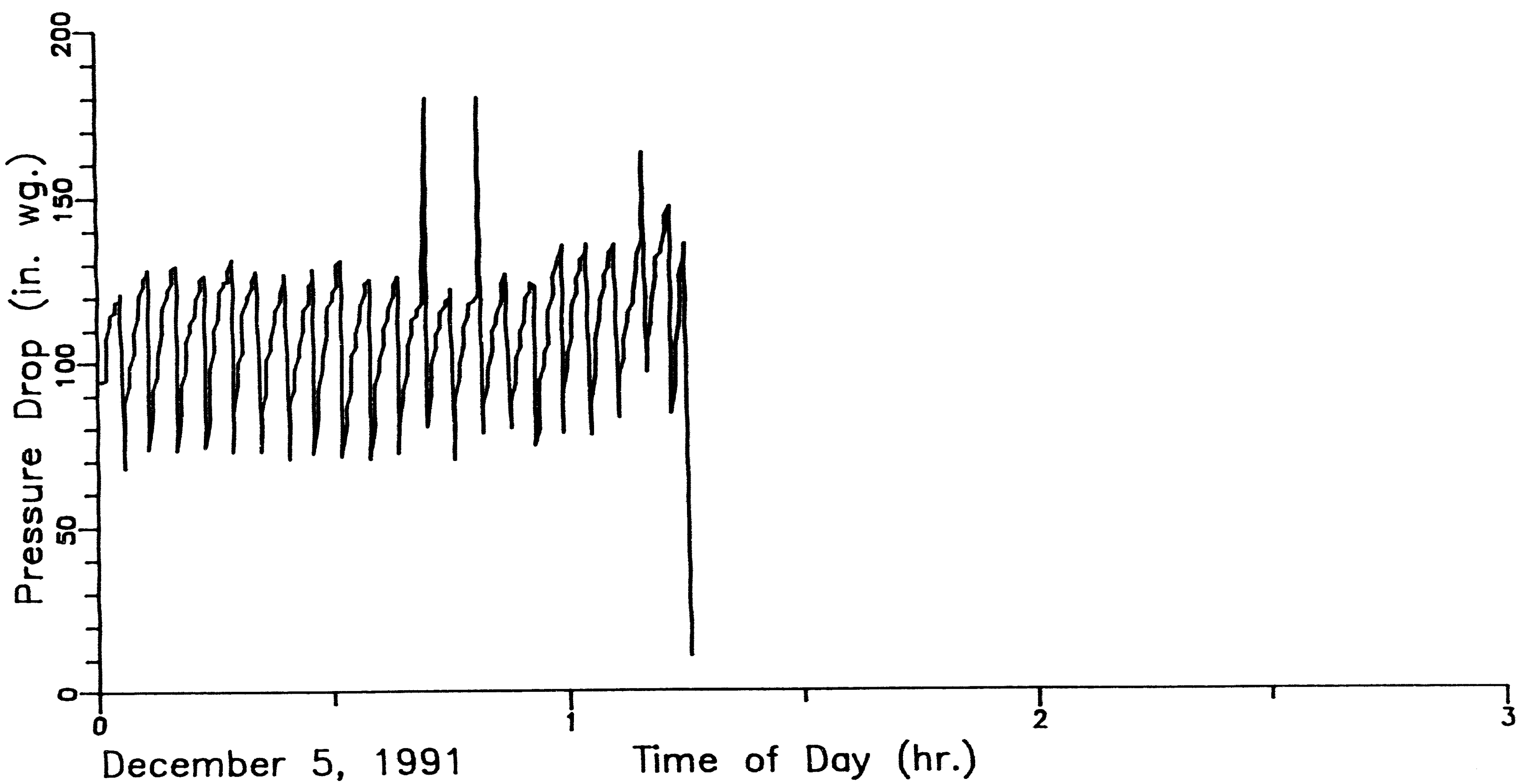

December 5, 1991

0115 Flow to filter stopped (Bypass valve opened)

Figure 4

Texaco Filter Performance Data

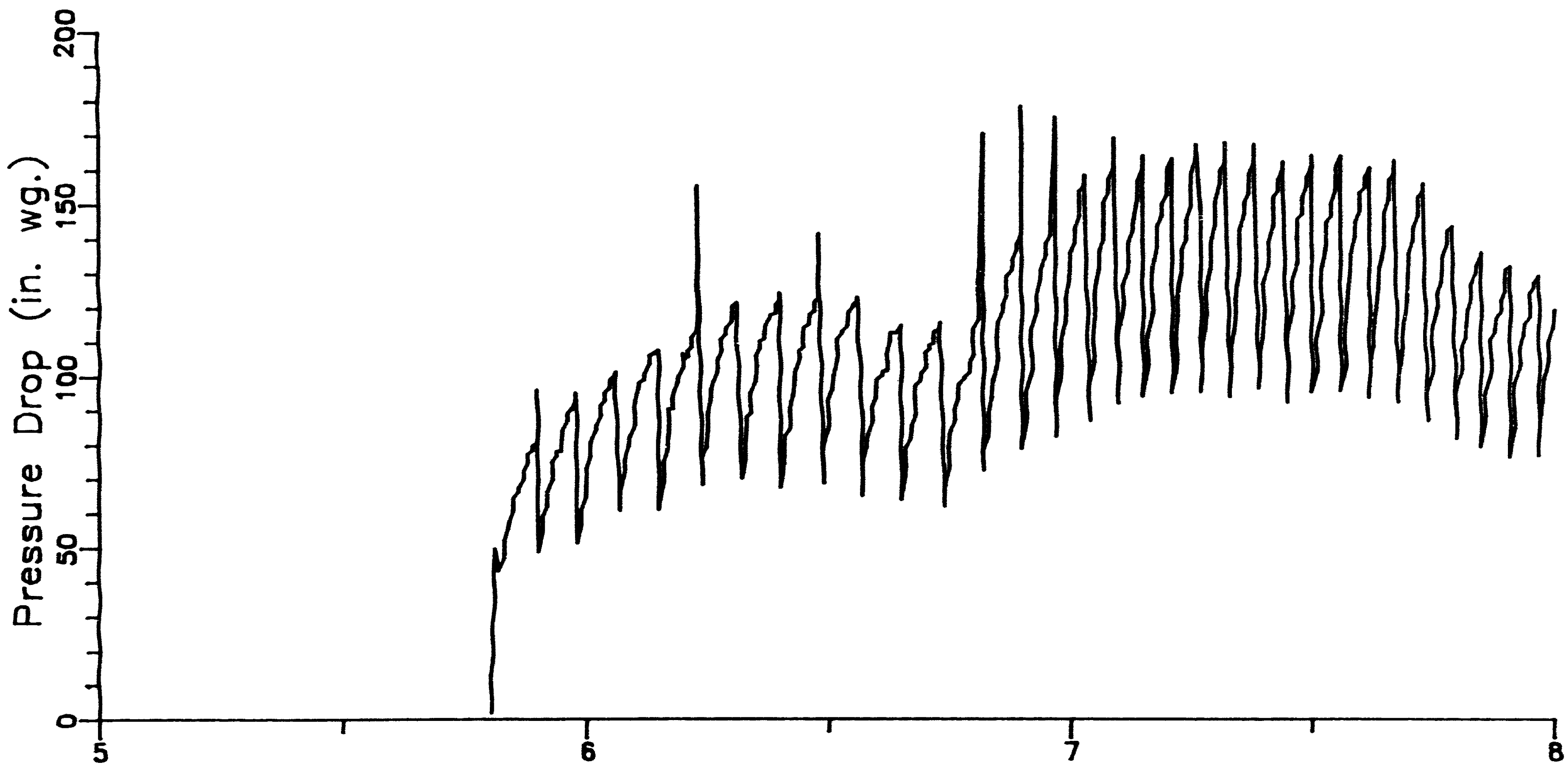

December 5, 1991

0548 Flow Restarted to filter

Figure 5

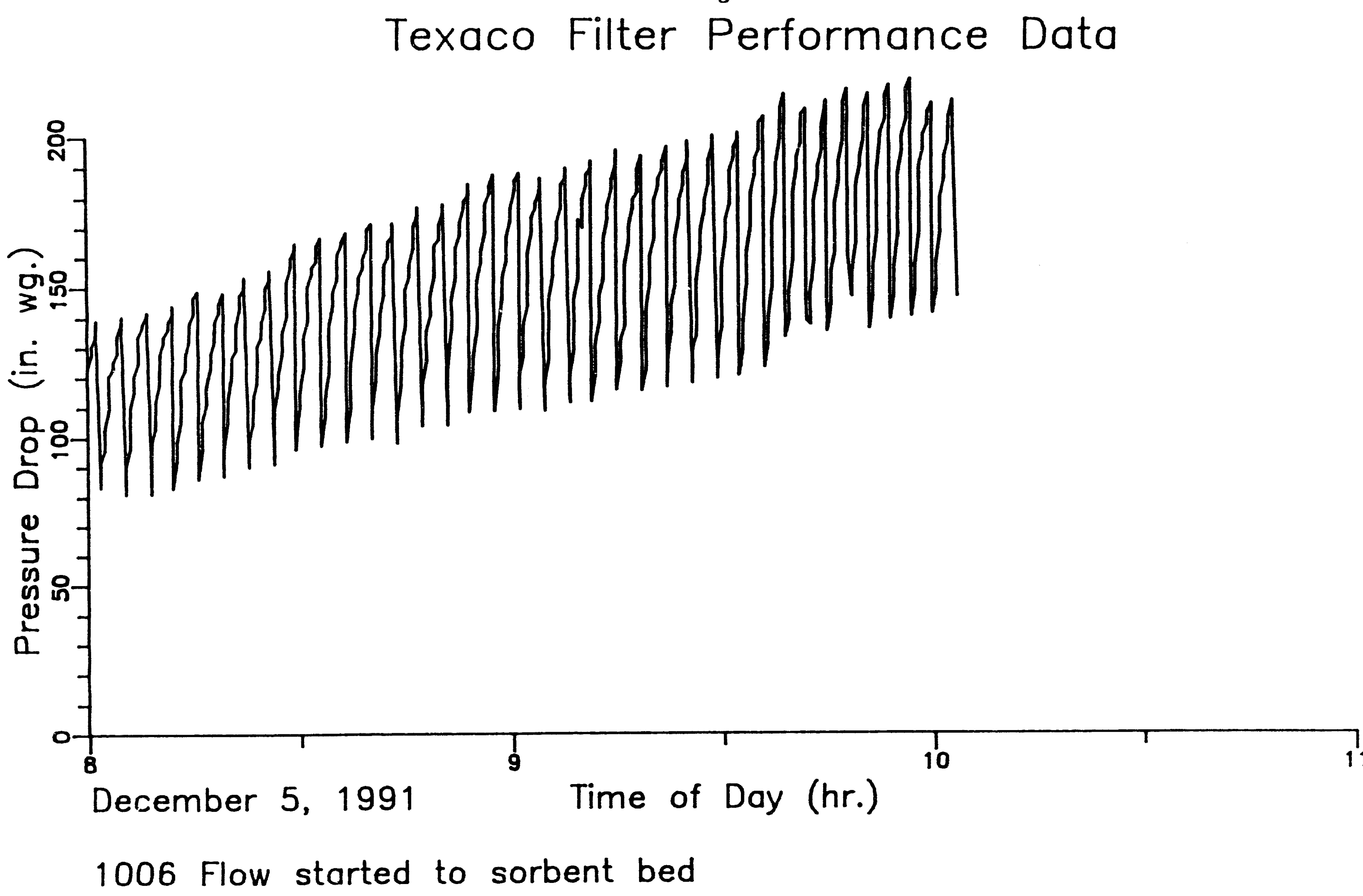
Texaco Filter Performance Data
Pressure Drop (in. wg.)
0
50
100
150
200
8
9
10
11
December 5, 1991
Time of Day (hr.)
1006 Flow started to sorbent bed

Figure 6

Texaco Filter Performance Data

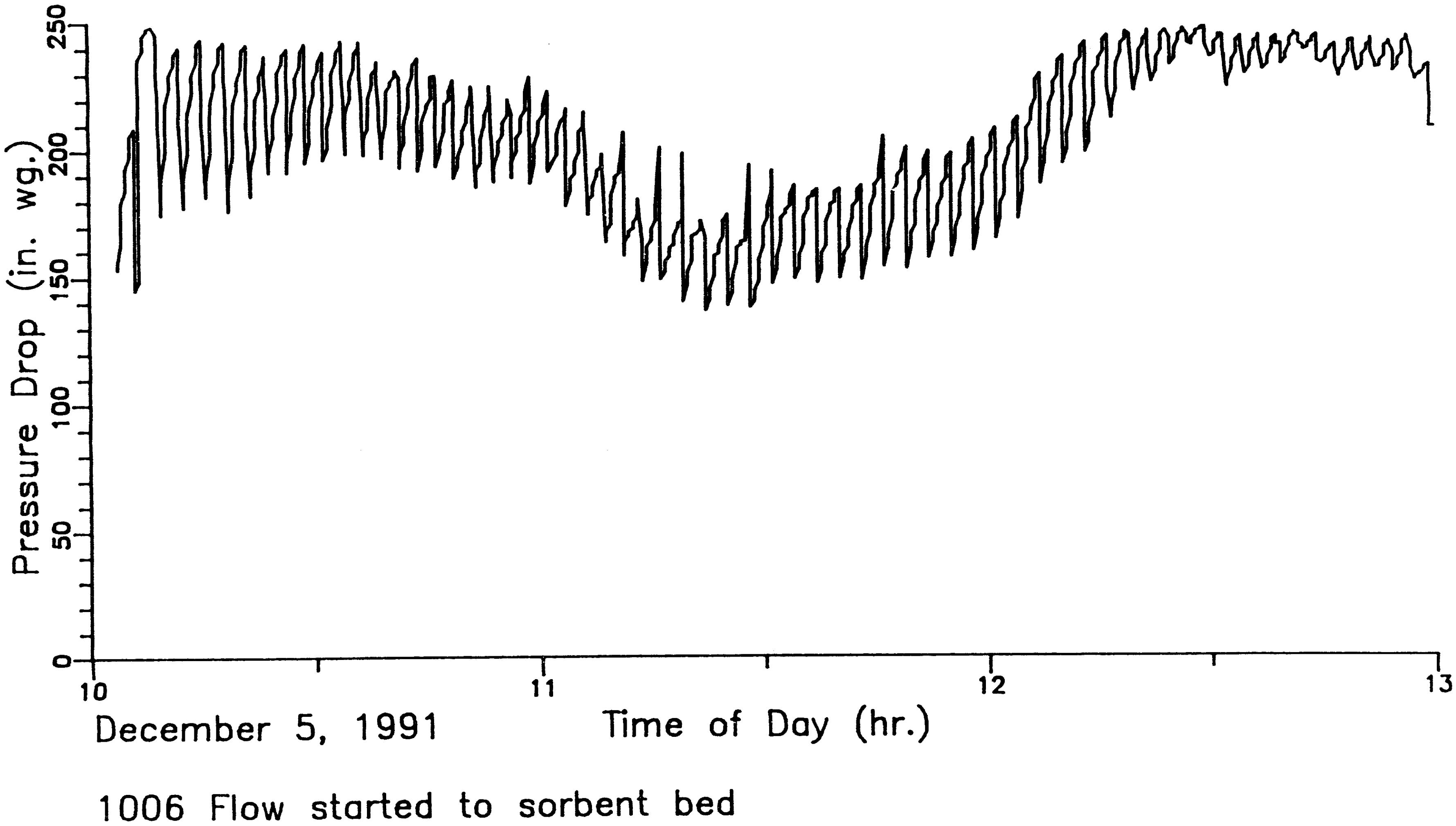

Figure 7

Texaco Filter Performance Data

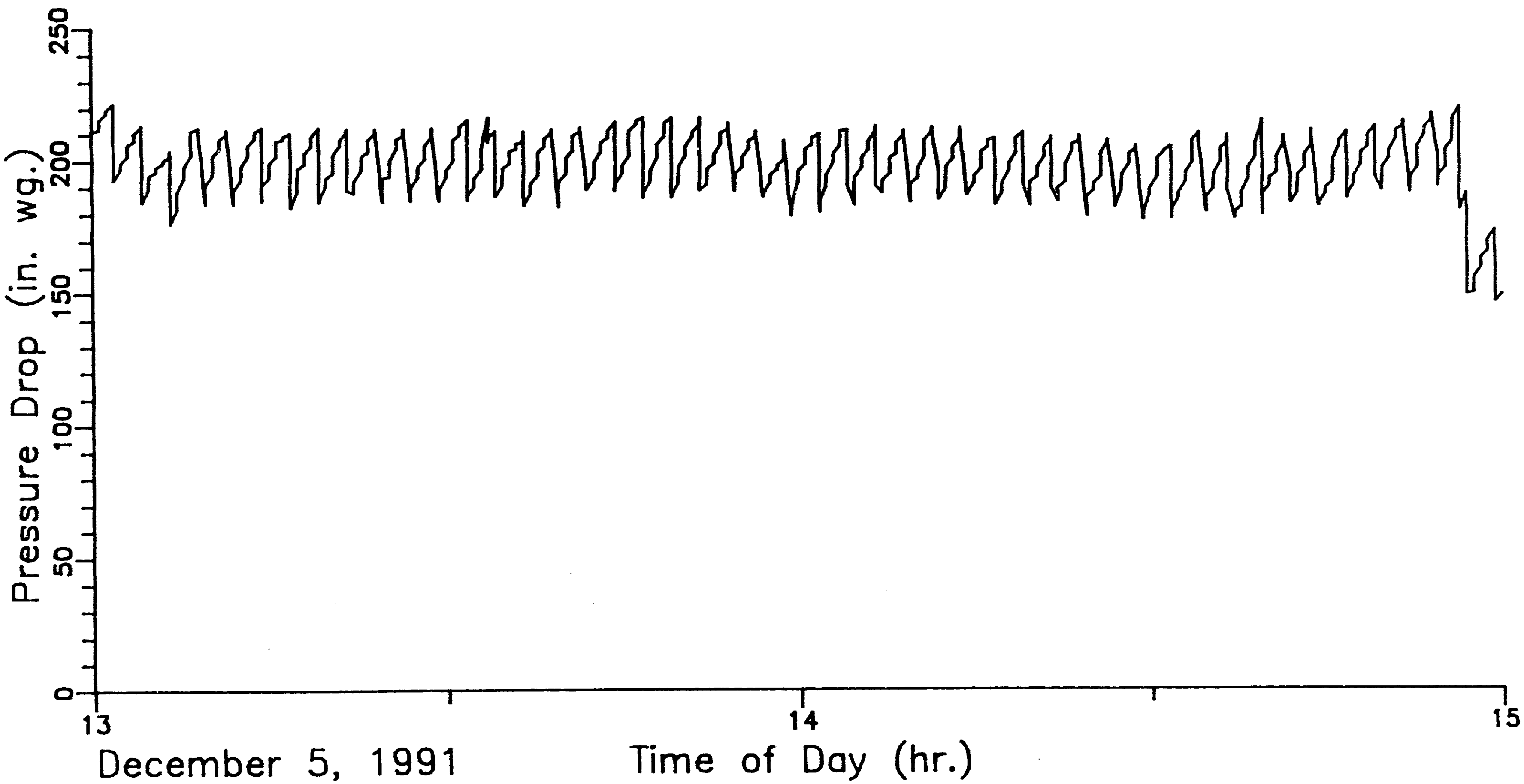

1500 Flow to sorbent bed stopped

Figure 8

Texaco Filter Performance Data

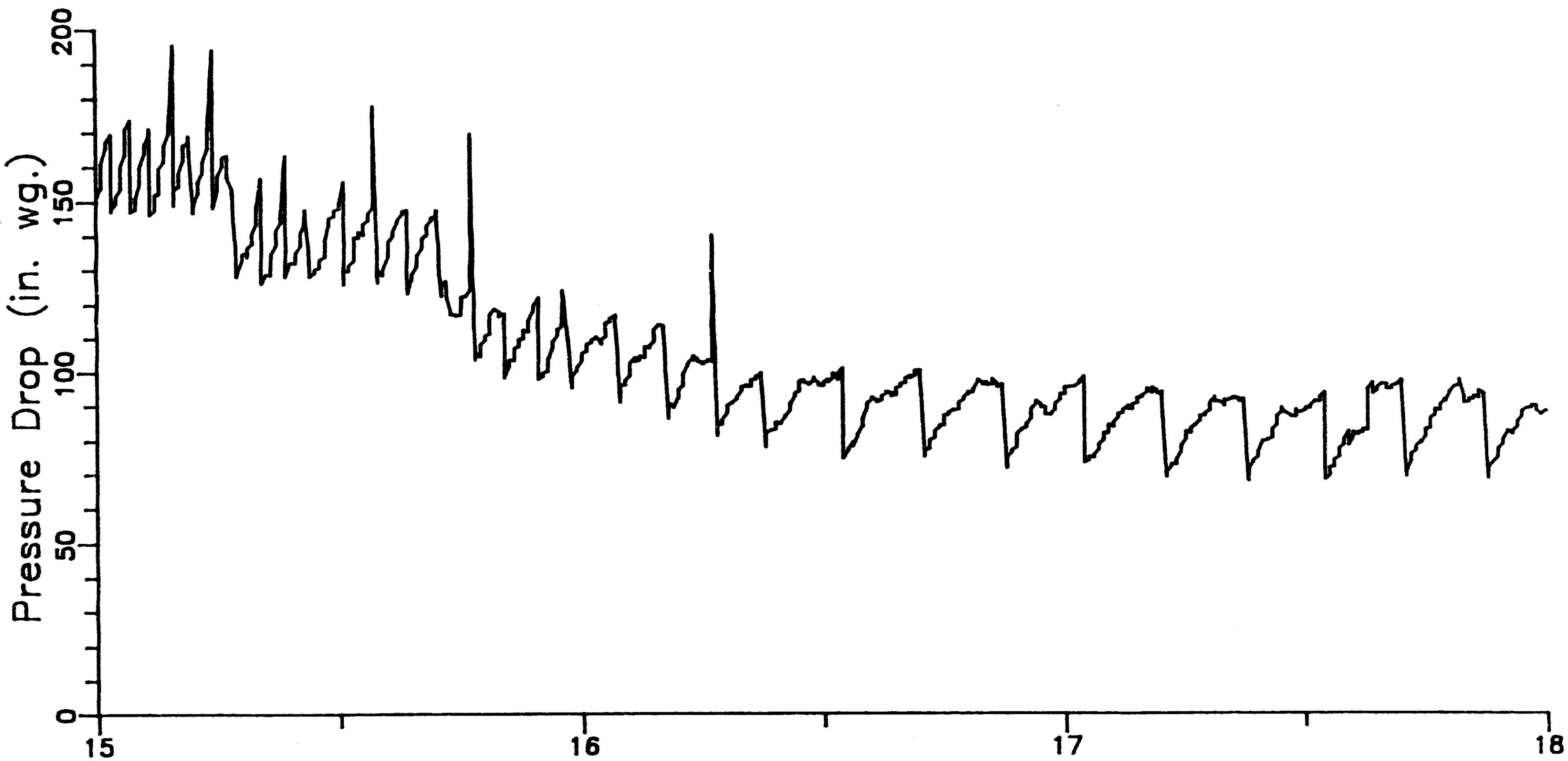

December 5, 1991 Time of Day (hr.)

1500 Flow to sorbent bed stopped

Figure 9

Texaco Filter Performance Data

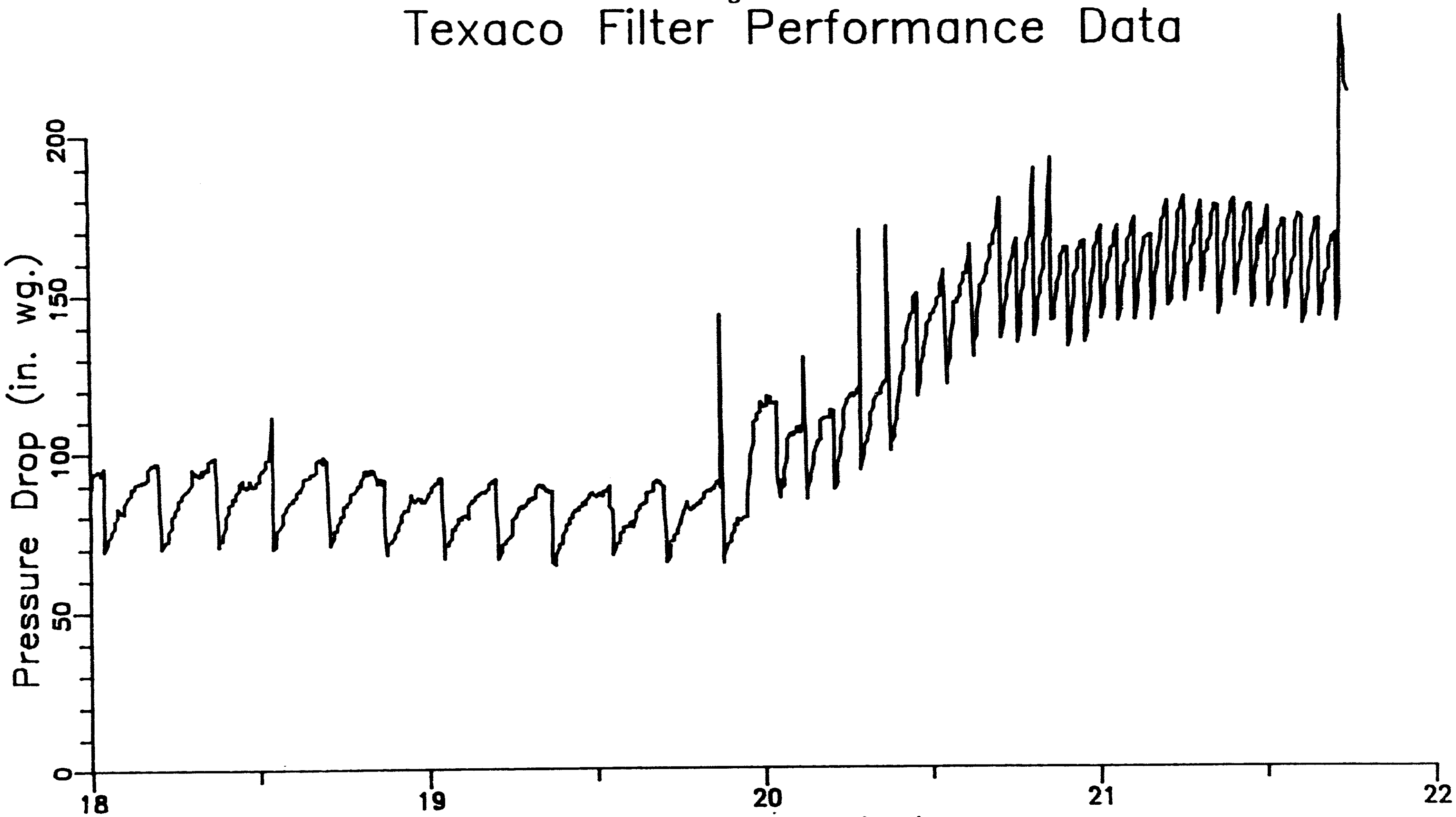

December 5, 1991

2145 Flow started to sorbent bed

Figure 10

Texaco Filter Performance Data

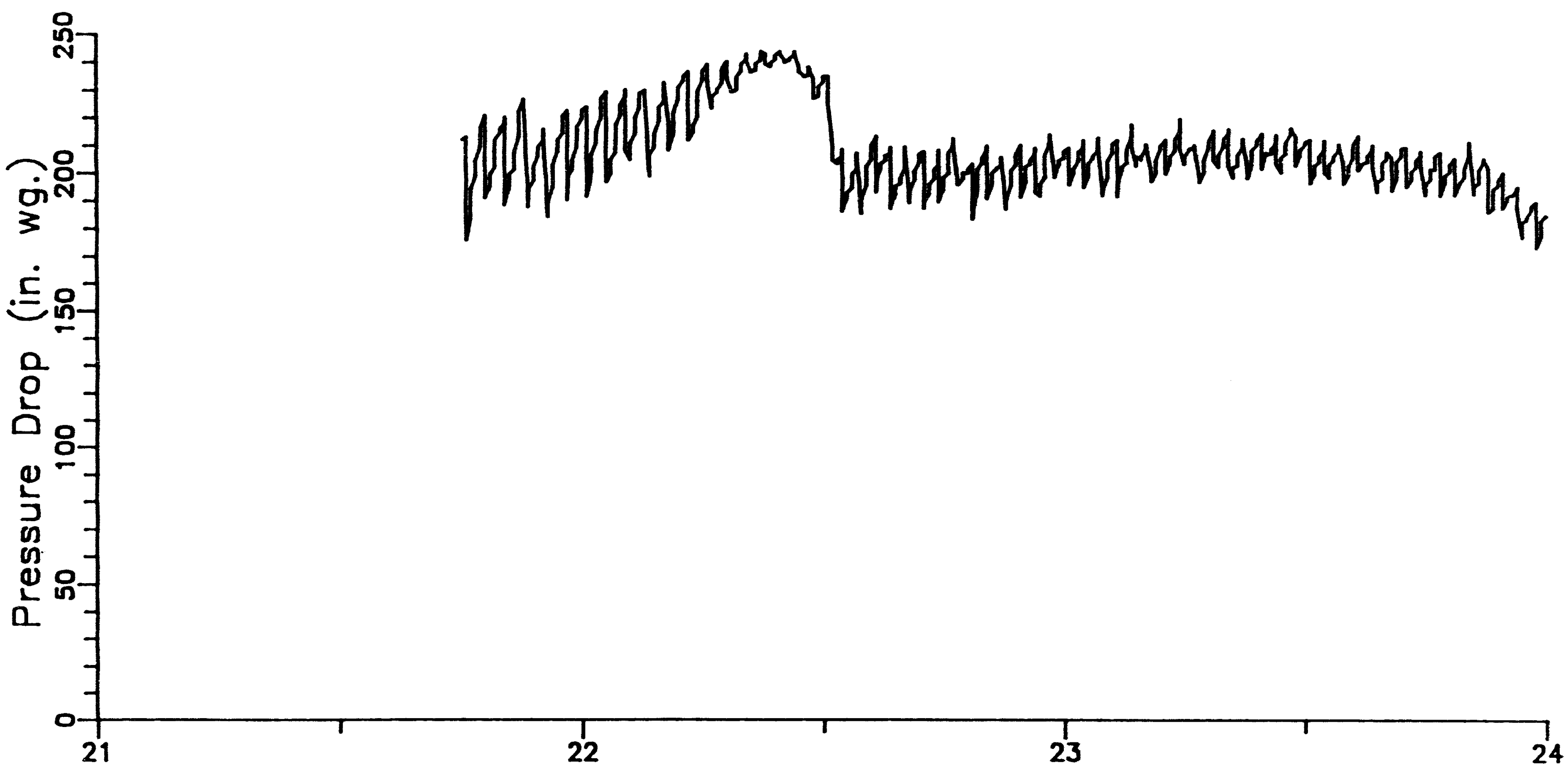

December 5, 1991

2145 Flow started to sorbent bed

Figure 11

Texaco Filter Performance Data

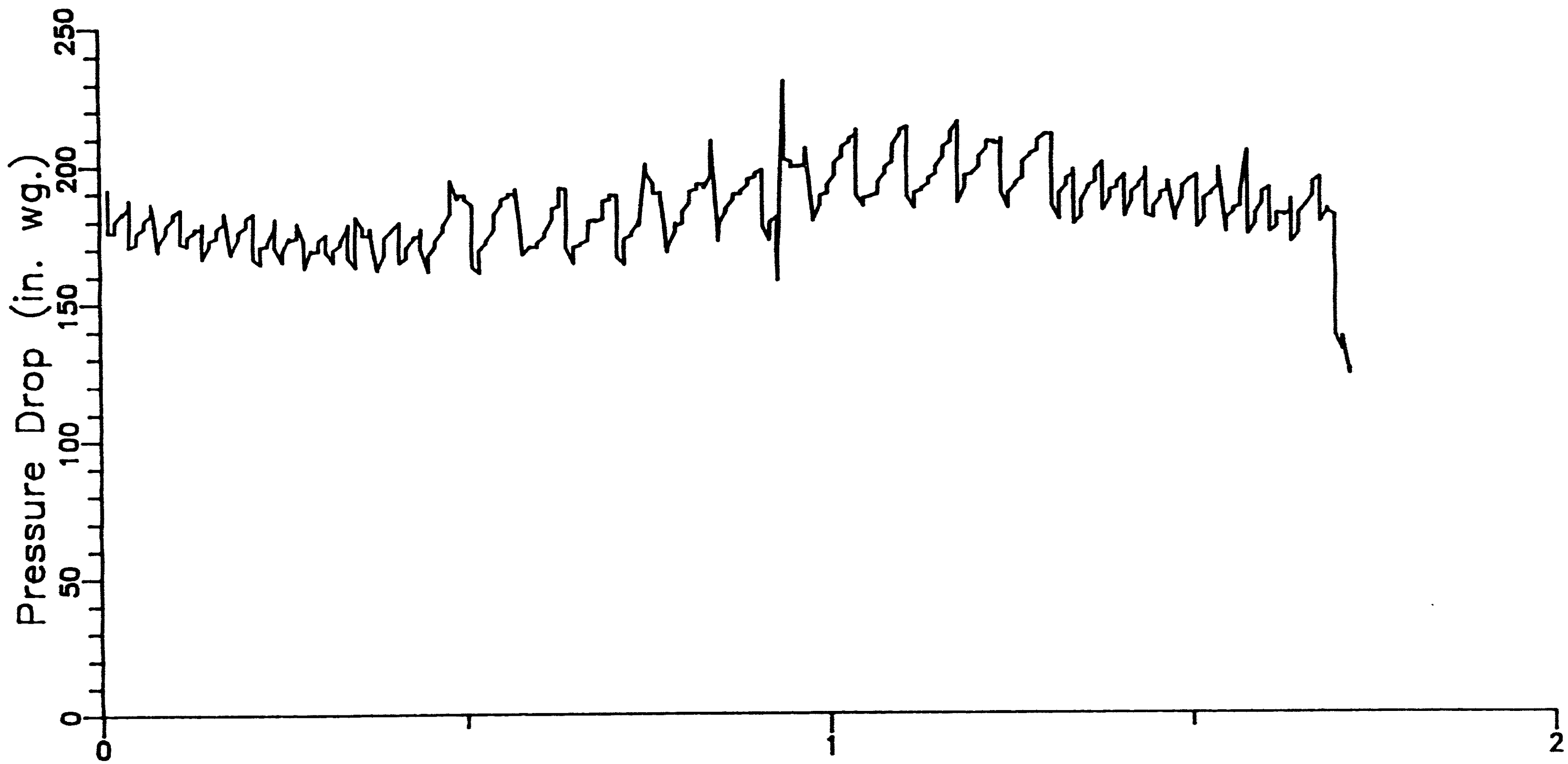

0143 Flow to sorbent bed stopped

Figure 12

Texaco Filter Performance Data

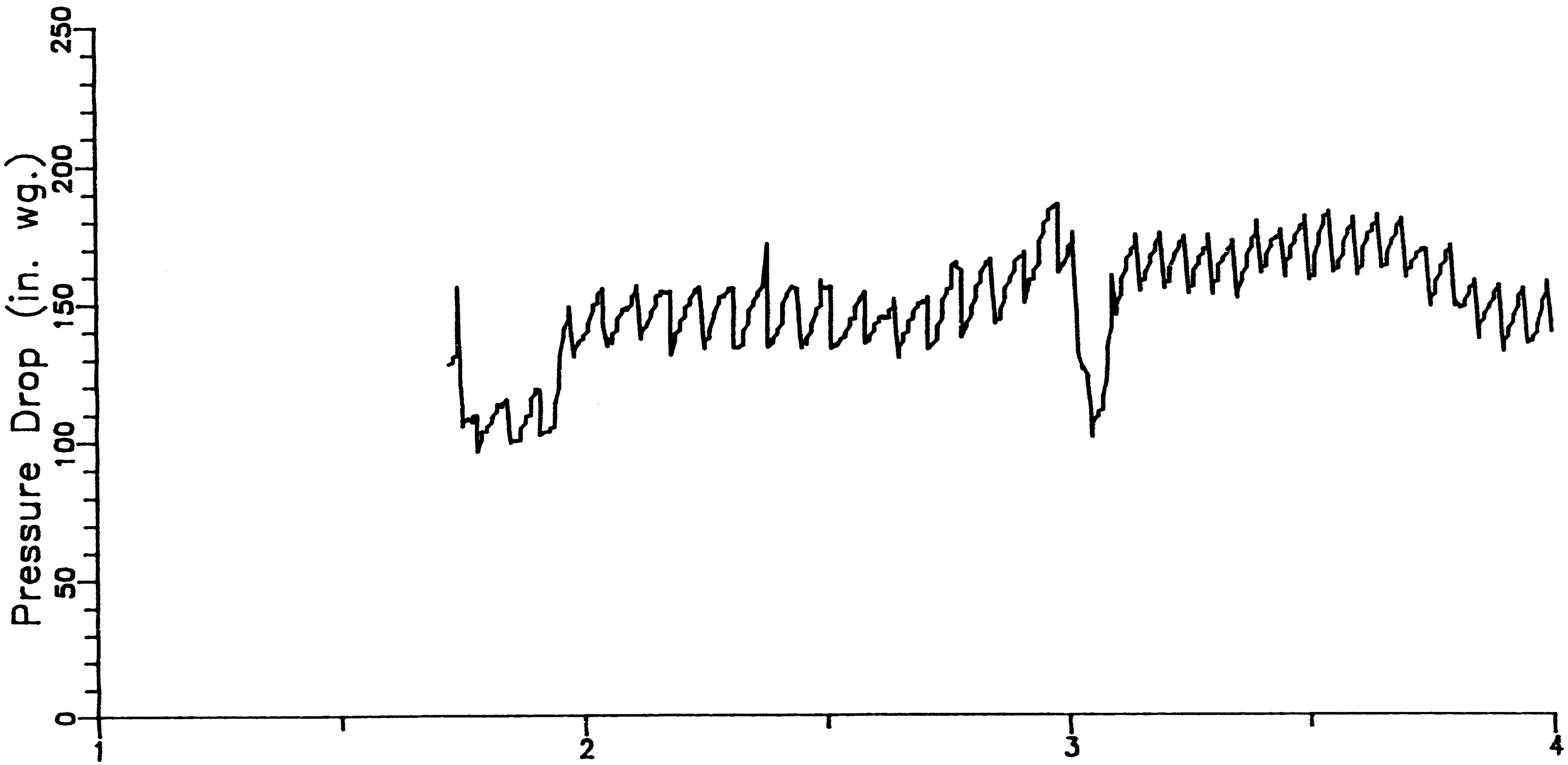

December 6, 1991

0143 Flow to sorbent bed stopped

Figure 13

Texaco Filter Performance Data

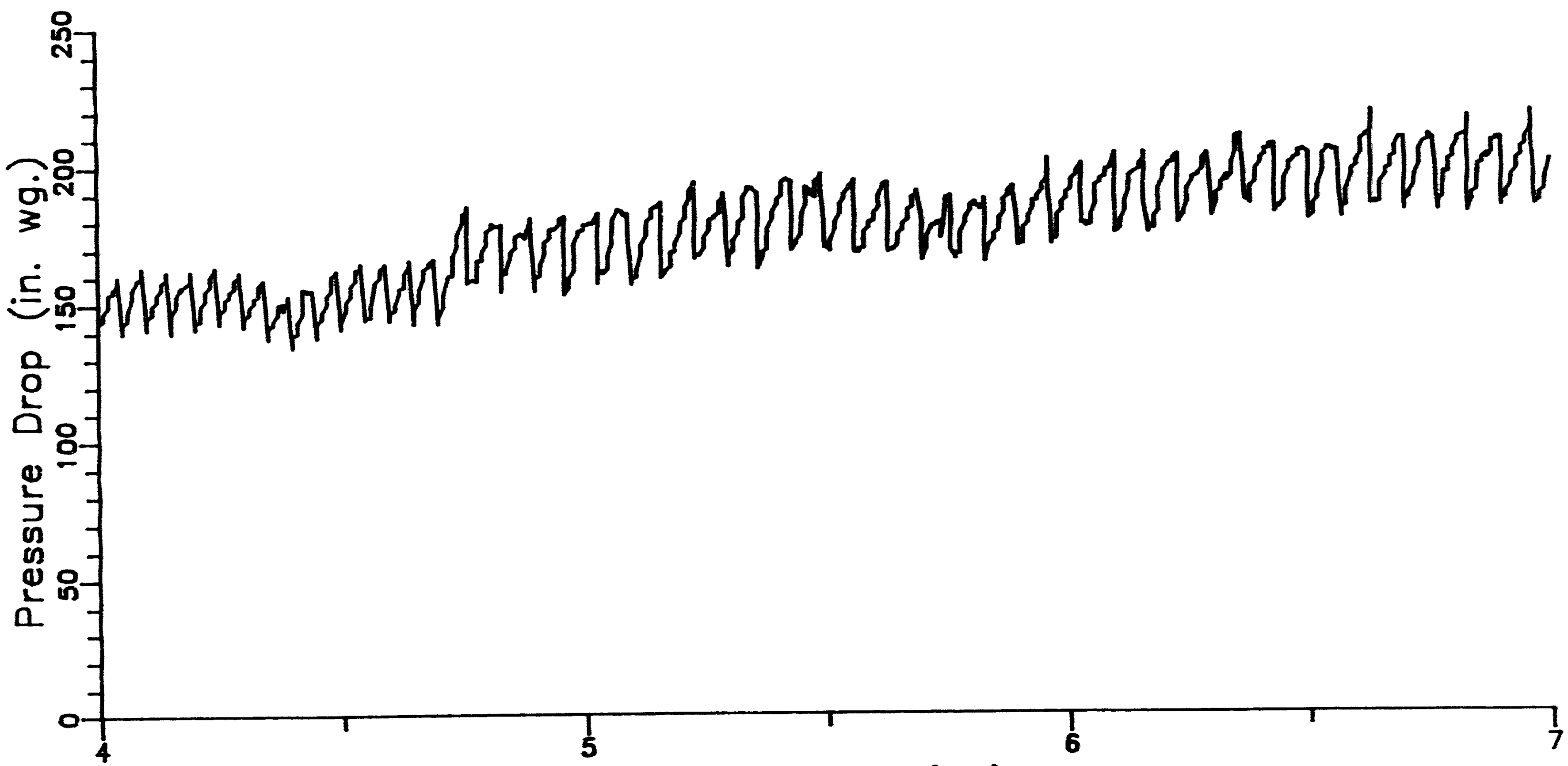

Figure 14

Texaco Filter Performance Data

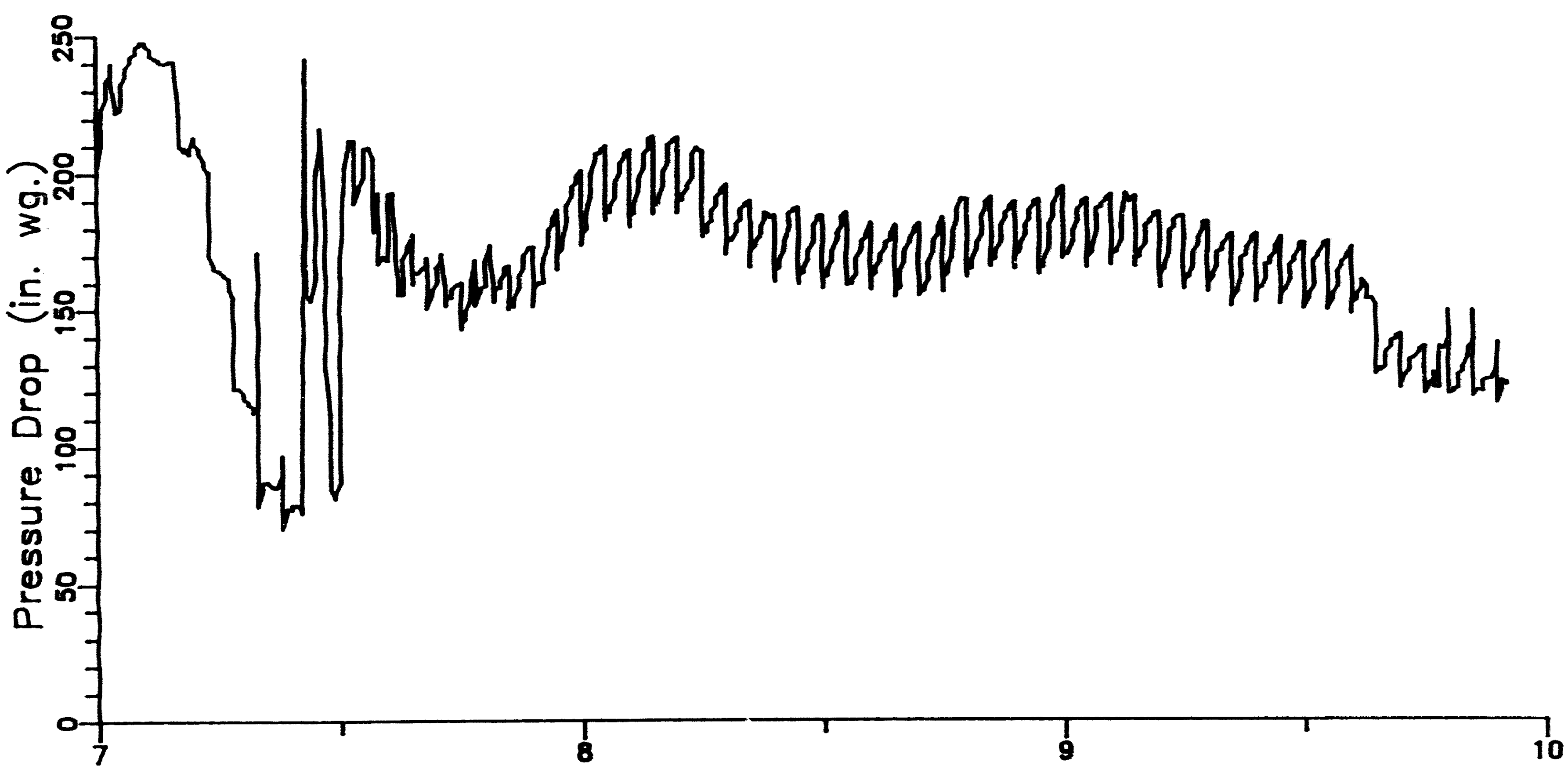

0955 Flow started to sorbent bed

Figure 15

Texaco Filter Performance Data

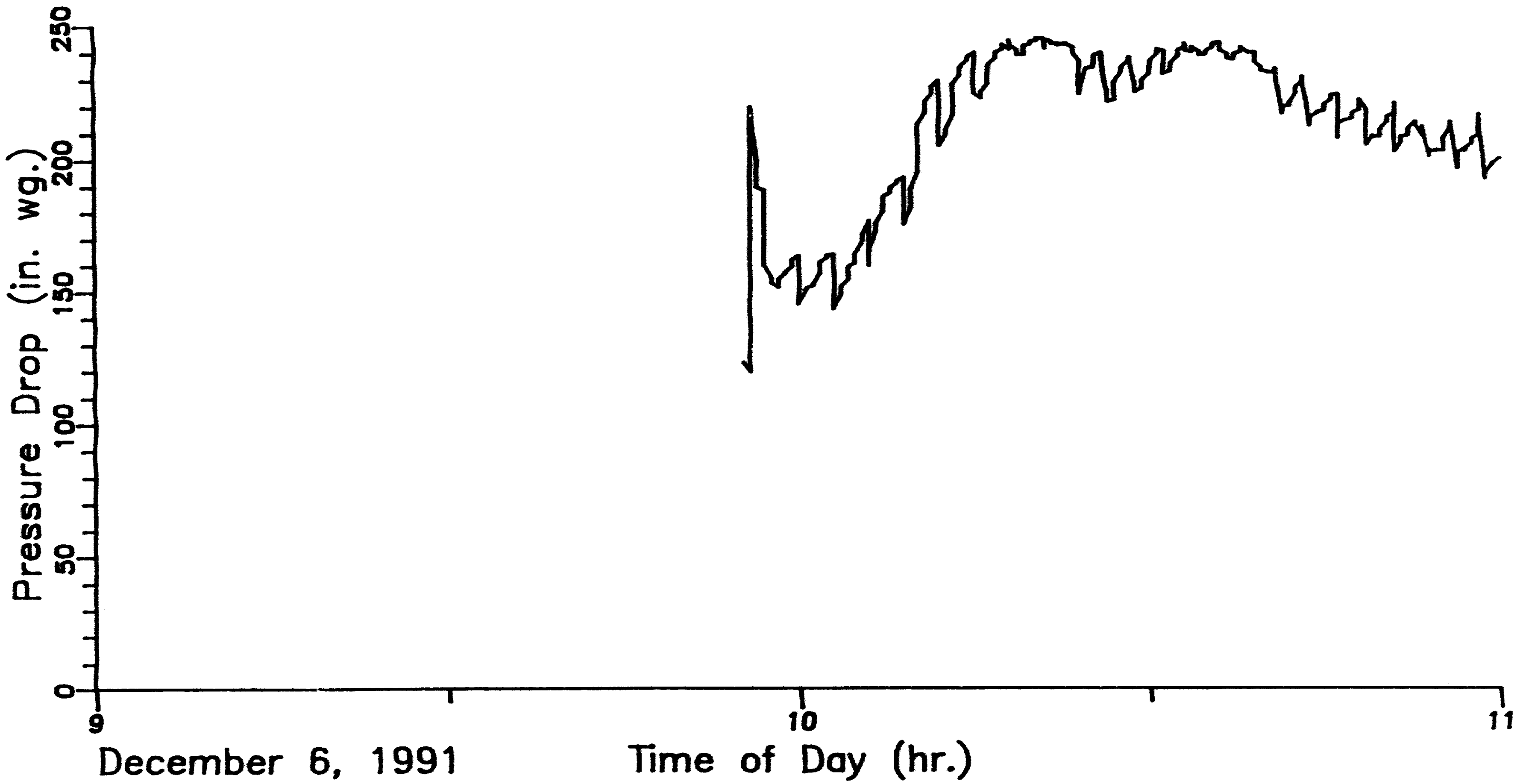

0955 Flow started to sorbent bed

Figure 16

Texaco Filter Performance Data

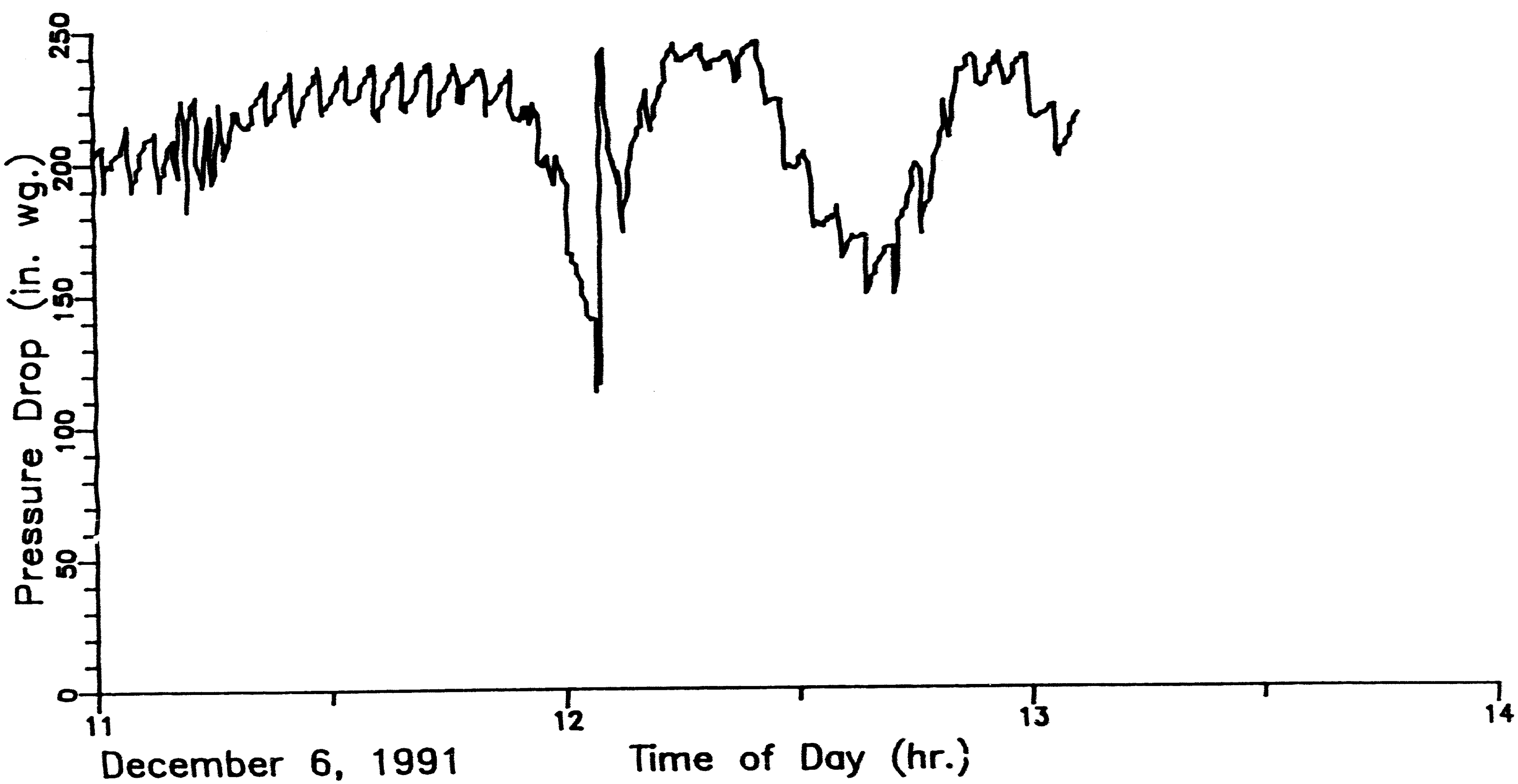

1311 Flow to sorbent bed stopped

Figure 17

Texaco Filter Performance Data

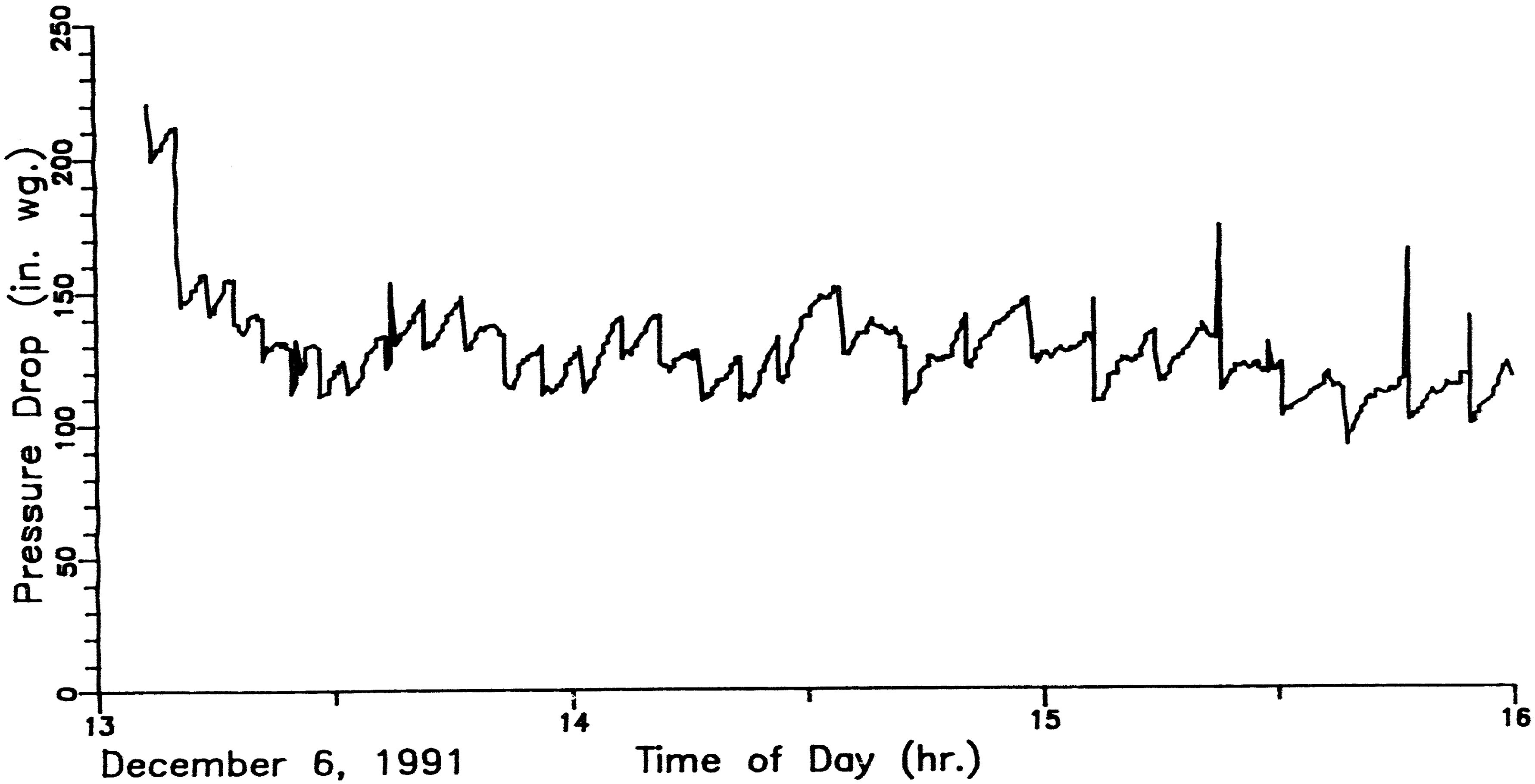

1311 Flow to sorbent bed stopped

Figure 18

Texaco Filter Performance Data

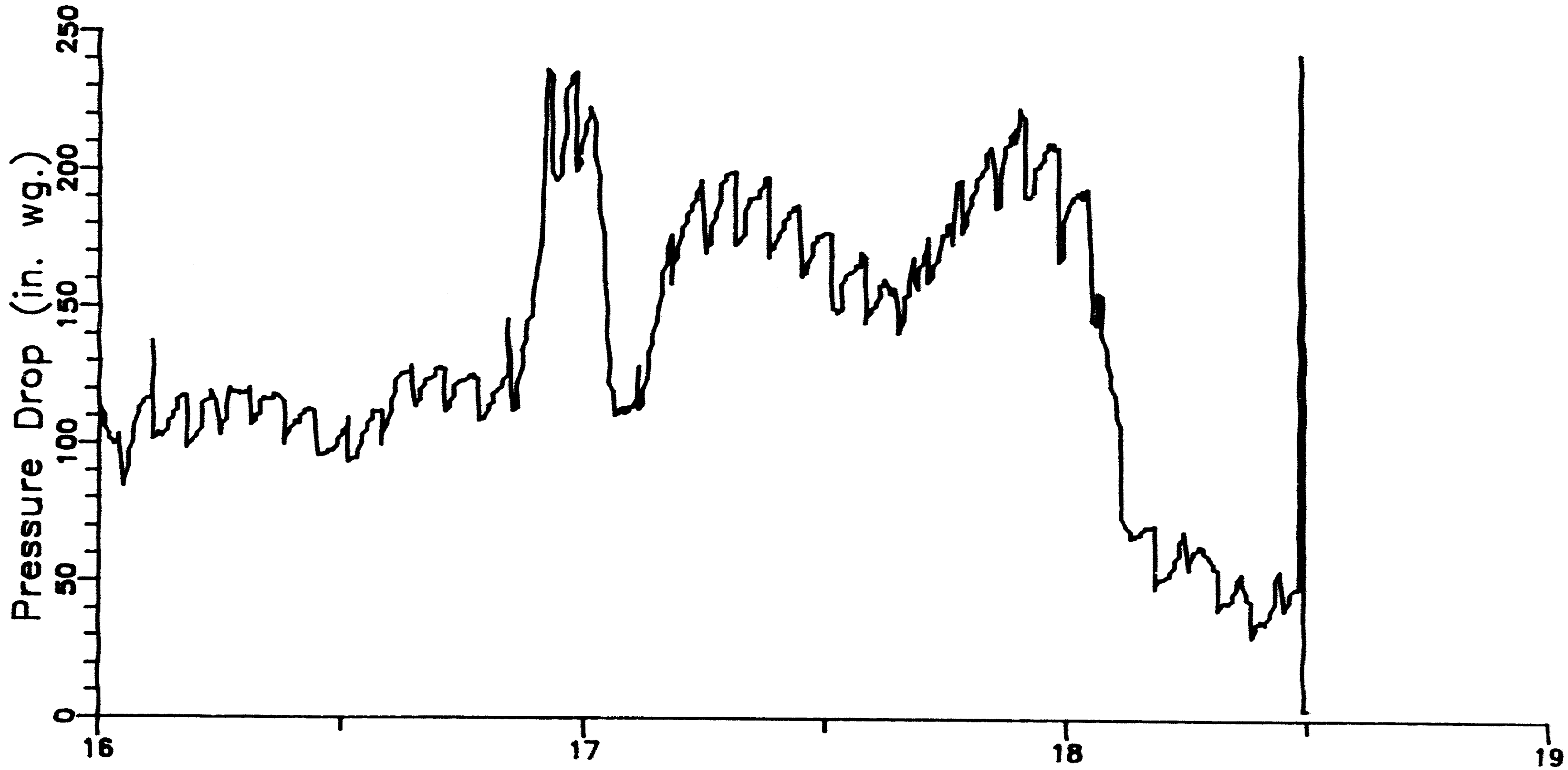

December 6, 1991

1825 System flow off

1830 System down

Figure 19

Texaco Filter Performance Data

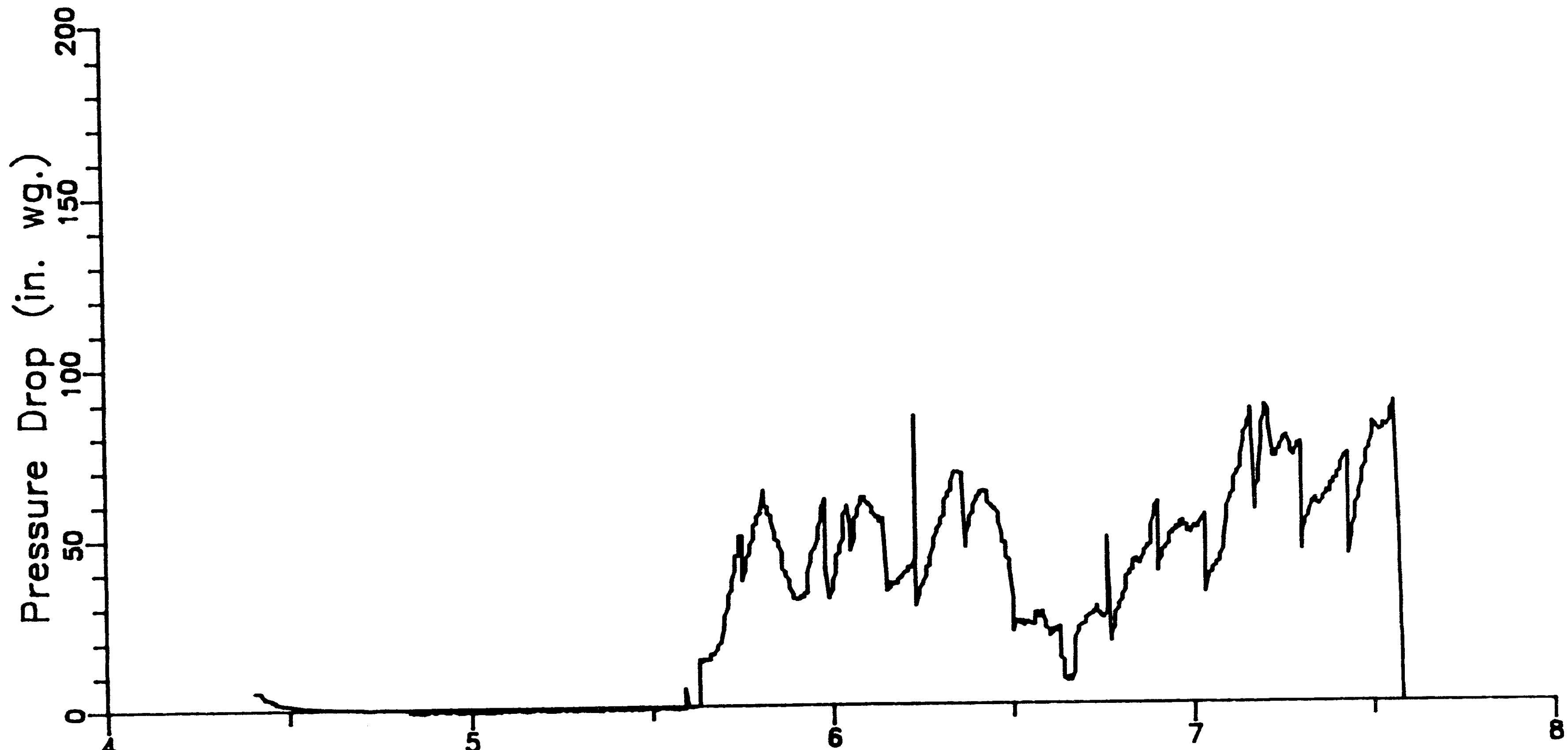

December 7, 1991
0424 Light–off
0537 Flow started to filter
0734 Flow to filter stopped

Figure 20

Texaco Filter Performance Data

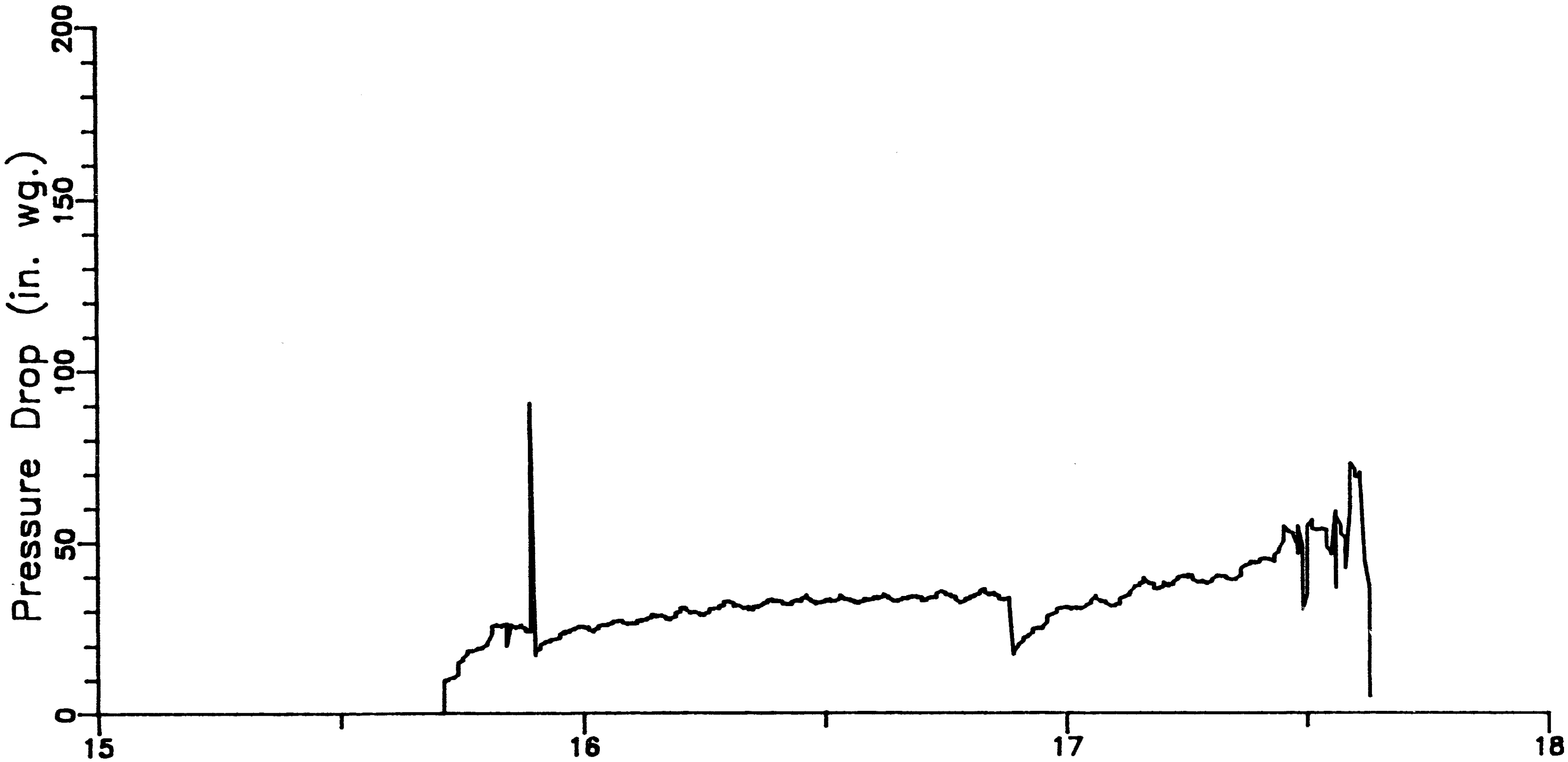

December 7, 1991

1542 Flow Restarted to filter system
1737 Flow to filter stopped
2145 Shutdown